ARMY RESEARCH LABORATORY

Causes of Electromagnetic Radiation From Detonation of Conventional Explosives:

A Literature Survey

Jonathan E. Fine and Stephen J. Vinci

ARL-TR-1690 December 1998

Army Research Laboratory

Adelphi, MD 20783-1197

ARL-TR-1690 **December 1998**

Causes of Electromagnetic Radiation From Detonation of Conventional Explosives:

A Literature Survey

Jonathan E. Fine and Stephen J. Vinci

Sensors and Electron Devices Directorate

Abstract

A literature survey was conducted on the presence of electromagnetic radiation from the detonation of conventional explosives. This survey is part of a technology effort to identify a useful battlefield signature that an individual soldier could detect. Sources reported observations of such signals in the range from as low as 0.5 Hz up to 2 GHz. Several of the investigators believed that the likeliest cause was charged particles created by ionization within the explosive region. The frequencies of the radiation appear related to the duration of shock waves and other hydrodynamic phenomena caused by the detonation. A calculation model presented in the literature provides estimates of frequency bands in this range and also of signal levels produced. The model is used to analyze some of the published results and provide some correlation between observations of several investigators.

Contents

Figures

Tables

1. Introduction

1.1 Background and Purpose of Investigation

The Sensor Integration Branch has investigated the emission of electromagnetic (EM) radiation during detonations of conventional explosives. This investigation is part of a technology effort to identify a wide range of battlefield objects of interest to the individual soldier. The program's ultimate objective is to provide a passive, portable, self-contained unit that can use multisensor inputs to detect, locate, and identify sources of weapons fire and explosives detonation. In the first year (FY 96), the branch surveyed related work reported in the literature to determine the signal levels and frequencies to be expected and to understand the causes of this radiation.

Electromagnetic radiation from conventional explosives originates from several sources [1] as seen in figure 1. Radiation is emitted from projectile travel in the launch tube, muzzle blast after projectile exit, discharge of electrostatic buildup on a projectile in flight, detonation at target, and impact of metallic fragments at target. The characteristics of radiation from each of these scenarios may be different. We theorize that the radiation from tube-launched weapons such as small arms, mortar, and artillery will exhibit different characteristics from bomb or projectile detonations. Their differences are because of the presence of tube walls, which may conduct charged particles while concentrating the expanding propellant gases in one direction.

We might expect that, whatever the source, the radiation should be related to the duration and intensity of the explosive event. The likelihood of detecting the radiation will be affected by the source's proximity to various types of materials, such as metals (gun tubes, baseplates, shell

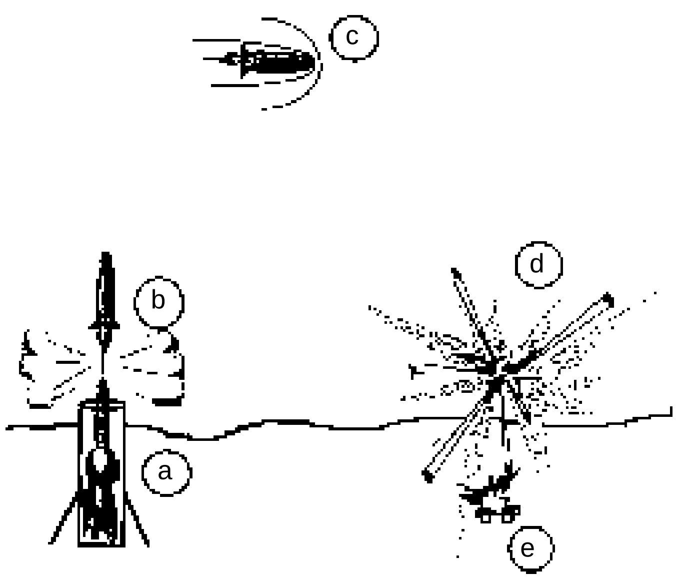

Figure 1. Sources of radiation from launch to detonating: (a) projectile travel in the launch tube, (b) muzzle blast after projectile exit, (c) discharge of electrostatic buildup on a projectile in flight, (d) detonation at target, and (e) impact of metallic fragments at target.

fragments) and nonmetals (earth, air, moisture content), and the presence of ambient electric and magnetic fields.

1.2 Overview of Literature Survey

We began this study with an extensive literature search. Much of the material was old—1958 to 1975—but provided a good basis for understanding the types of signatures that might be expected from muzzle blast, projectile travel, or detonation on target. Most of the papers found did not offer a solid theoretical explanation of the detectable radio frequency (rf) energy but mostly reported experimental findings. Our main interest in reviewing the papers was to establish the kinds of signals detected, the frequencies and signal levels observed, and any insight into the possible sources of radiation.

Several researchers who have detected EM energy associated with battlefield munitions [1–4] observed signals in a wide range of frequencies, as summarized in table 1. The signals are from 0.5 Hz to 1 GHz. The frequency affects signal propagation and detectability, as discussed in section 3. In addition, Takakura and Curtis report delays from initiating the explosive to detecting a signal from 20 to 160 µs and as long as 2 s. Curtis also reports a low-frequency (LF) signal that lasted 15 to 19 s, which is beyond the duration of any conceivable explosive event.

Table 1. Summary of significant findings.

Source	Frequencies	Possible cause
Trinks 1976	1–100 kHz	Ionization of gas at muzzle
	2 MHz–1 GHz	Discharge of projectile upon impact at target
Takakura 1955	6–90 MHz	Ionization at shock front of explosion
Stuart 1975	250 MHz–1 GHz	None given, experimental results only
Curtis 1962	0.5–350 Hz	None given, experimental results only

2. Literature Survey

A review of the literature revealed attempts to detect EM radiation from conventional explosives from the late 1950s to the present. Most of the papers reported experimental findings that showed an effect, but did not provide enough documentation to establish the field levels. They also provided some physical insight and conjectures on what the causes of the radiation might be, but did not attempt to offer a solid theoretical explanation of the detectable rf energy. We reviewed this literature to establish what frequencies and signal levels were observed and to determine the possible sources of radiation.

2.1 Trinks

Trinks and his colleagues in Germany, who wrote several reports in German, laid much groundwork. At one time, Trinks visited the Harry Diamond Laboratories* and lectured on his work. The lectures were compiled into an internal report that is cited in the next paragraph, along with other reports that he and his associates wrote.

In Trinks' 1976 report [1], he discusses the presence of several aspects of radiation caused by detonations:

- rf (10 MHz–2 GHz) radiation upon detonations possibly because of "microsparks" caused by charge equalization of fragments,
- strong LF (1–100 kHz) radiation caused by muzzle flash possibly because of the ionization of gases near the muzzle, and
- the electrically charged state of projectiles and the subsequent detection of high frequency (HF) (2 MHz–1 GHz) pulses on impact at the target.

An electrostatic charge builds up on a projectile in flight because of many competing factors such as triboelectric effects (which can occur whenever materials in a projectile's path, such as dust or water particles, are stripped across the surface by the airstream), charged particles impinging on the projectile surface, electric fields caused by shock waves, the projectile passing through the muzzle flash region, and the presence of a reacting tracer. A limiting value of charge is reached above that which charge carriers discharge by spraying off the projectile. This is known as corona discharge. Theoretical calculations of charge on a projectile in flight show good conformity to those determined experimentally, as shown in figure 2. Trinks provides experimental evidence for several of these effects, but he does not provide clear mathematical relationships relating the charge buildup to known or measurable quantities.

*Now part of the Army Research Laboratory.

Figure 2. (a) Measured and (b) computed signals obtained by application of ring-shaped sensor. Projectile's charge is assumed as a line charge, and *v* is velocity of projectile or line charge.

[Reprinted with permission (see ref 5)]

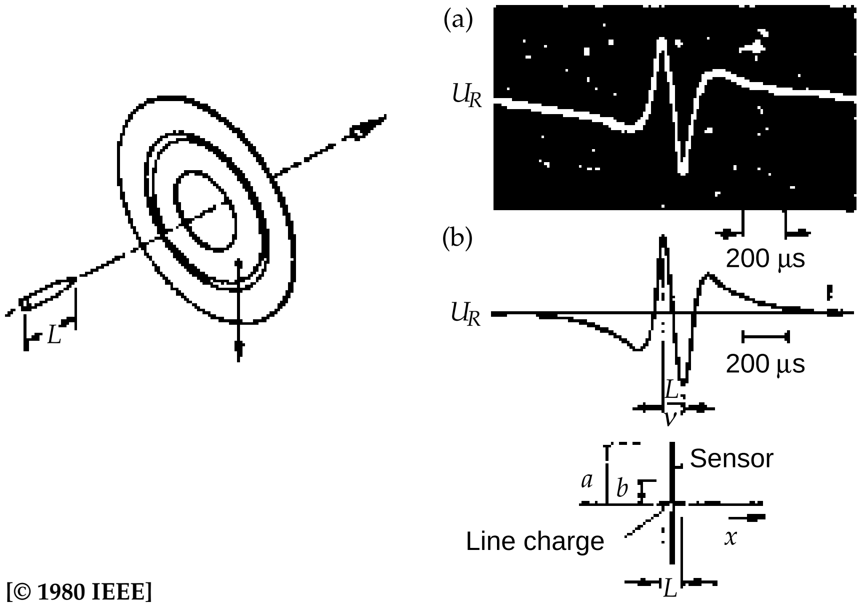

[© 1980 IEEE]

Trinks and ter Haseborg include a summary of the many experiments and their results in a 1980 IEEE transactions report [5]. They mention that even though the physical mechanism leading to the presence of signals is very complex, the origination and separation of electrical charges are fundamental reasons for all the effects observed.

2.2 Takakura

Takakura [2] presents experimental measurements of EM radiation at frequencies of 6 to 90 MHz upon detonation of explosives by using burning paper as the igniter. This method of ignition was used to prevent changes in the detected radiation, which sometimes occurs when firing by electrical means. It was observed that the signal amplitude is porportional to $1/r$, where r is the distance from the source of the radiation to the observation point. This variation corresponds to the decrease in signal that occurs with EM radiation in the far field. Nonradiative fields decrease faster than $1/r$. Decreasing signal strength was also found for increasing frequency. Notably, these tests showed an extremely high correlation between simultaneous signals from two different antennas both set up parallel or perpendicular to each other near the explosion. Takakura offers no clear reason for the detection of such signals but suggests the possible cause to be linked to the ionization at the shock front. Takakura also observed that EM radiation pulses detected at frequencies below 90 MHz were delayed 80 to 160 µs from the start of the detonation.

2.2.1 Description of Experiment

Takakura detonated small explosives, 0.2 g of lead azide, on a wood base 30 cm above a concrete floor. He used a photocell as a trigger for

3300-, 190-, and 90-MHz receivers. Antennas of wires 50 to 160 cm in length and a horn were used and placed 10 to 200 cm from the explosive. He used burning paper as the igniter to prevent changes in the detected radiation, which sometimes occur when firing by electrical means. The peak light intensity occurred 20 to 30 μs after initiation of detonation, and pulses were detected on the 90-, 14-, and 6-MHz channels 80 to 160 μs after initiation of the explosives. The major part of the rf pulses occurred after the light emission had decreased. He varied the explosive size from 0.1 to 0.4 g and found that the number and intensity of pulses increased with increasing mass.

2.2.2 *Results*

The signal strengths measured were in the tens to hundreds of microvolts, but Takakura did not provide *E*-field values in the body of the report. The range of *E*-field in V/m can be estimated by dividing the values of voltage obtained by the length in meters of the antenna being used. These results are presented in table 2.

In an appendix to his paper, Takakura uses "a typical impulsive noise detected experimentally" having an *E*-field value of 4×10^{-4} V/m to estimate the value of the acceleration of an ionized particle in an expanding gas cloud. The estimated *E*-field values from the table agree with this value, thus indicating that our method of estimation is reasonable.

2.2.3 *Estimation of Average Dipole Moment and Charge Acceleration*

Takakura attributed the detected radiation to acceleration of electrons that are ejected by ionization at the shock front produced by the detonation of the lead azide. In his appendix, he presents some quite sketchy calculations on the change of dipole moment induced at the shock front and the radiation produced by this effect. Since these calculations provide useful

Table 2. Estimate of *E*-field range from Takakura's voltage measurements from detonating 0.1 to 0.4 g of lead azide.

Bandwidth of instrumentation channel (MHz)	Antenna length from explosion (cm)	Distance measured (cm)	Range of voltages (V)	Range of calculated *E*-fields (V/m)
Video	100	40	10 mV	10^{-2}
6	150	40	20–200 μV*	13–133 μV/m
14	50	40	None given	None given
90	75	15	50–100 μV	66–133 μV/m
190	None given	10	None given	None given
330	None given	10	None given	None given

*In his paper, Takakura's statement "tens to several hundred microvolts" is ambiguous, so that these numbers represent the lower limits of the range detected.

benchmark numbers for the *E*-field near the detonation and the acceleration of the charges comprising the dipoles, we elaborated on Takakura's efforts by supplying what we believe may have been the missing steps and assumptions behind his calculations.

Takakura considers a region of dipoles distributed uniformly over the volume of the radiating region, which he takes to be a sphere of volume 10 cm^3 surrounding the explosive. The charge density for a singly ionized dipole is given by

$$\rho = en \quad , \tag{1}$$

where e is the unit of charge for a singly ionized dipole, 1.6×10^{-19} C, and n is the number of dipoles per cm^3, for which he uses a value of 10^{10} per cm^3. He considers the *E*-field at a radius of 0.4 m from the center of the explosion caused by an average dipole of moment

$$\vec{P} = \int_V \rho \vec{s} dV \quad , \tag{2}$$

where $\vec{s}$ is the vector distance from the center of the volume to a point at which dipoles exist. The implied assumption is that one end of each dipole is anchored at the center of the volume, and the other end is free to move. These moveable ends are distributed uniformly throughout the radiating region. The above integration is an estimate of the net dipole moment of the distribution. (Note that, if the distribution of dipoles is spherically symmetric, the net dipole moment, consequently the *E*-field, will be zero because of the cancellation of equal and opposite terms in the integration. If asymmetry is introduced, for example by proximity of the explosion to the ground, then there could be a net dipole moment.)

From equation (2) using a uniform density, we can express the dipole moment as the net charge times an average length as

$$\vec{P} = \int_V \rho \vec{s} \, dV = \rho \int_V \vec{s} \, dV = \rho V \vec{s}_{avg} = q \vec{s}_{avg} \quad , \tag{3}$$

where

$$q = \rho V = enV \quad . \tag{4}$$

Takakura uses the second time derivative of *P*, which can be obtained by differentiating equation (3):

$$\ddot{\vec{P}} = q \ddot{\vec{s}}_{avg} = q \vec{a} \quad , \tag{5}$$

where

$$\vec{a} \equiv \ddot{\vec{s}}_{avg} \tag{6}$$

is the average acceleration of the moveable end of the dipoles.

Dividing equation (5) by q gives the following formula for the average acceleration in terms of the second derivative of the polarization:

$$\vec{a} = \ddot{\vec{P}}/q \quad . \tag{7}$$

Takakura gives the E-field in terms of the polarization by

$$\vec{E} = -\ddot{\vec{P}}/4\pi\varepsilon_o c^2 R \quad . \tag{8}$$

Solving equation (8) for the second time derivative of the polarization gives

$$\ddot{\vec{P}} = -4\pi\,\varepsilon_o c^2 R\vec{E} \quad , \tag{9}$$

where $\varepsilon_o = 8.85$ pF/m, and $c = 3.00 \times 10^8$ m/s.

In an appendix to his paper, Takakura gives a typical measured value for the E-field of 4×10^{-4} V/m. Using this in equation (8) at a distance of 40 cm from the center of the explosion gives for the second time derivative of the polarization

$$\ddot{\vec{P}} = 1.6 \times 10^3 \text{ C m/s}^2 \quad . \tag{10}$$

Using 10^3 cm^3 as the volume of the radiation source in equation (4) estimates the total polarization charge as

$$\begin{aligned} q = enV &= 1.6 \times 10^{-19} \text{ C/particle} \times 10^{10} \text{ particles/cm}^3 \times 10^3 \text{ cm}^3 \\ &= 1.6 \times 10^{-6} \text{ C} \quad . \end{aligned} \tag{11}$$

Substituting equations (10) and (11) into (7) estimates the value of acceleration as 10^9 m/s^2.

2.2.4 *Conclusions From Review of Takakura's Paper*

The main objectives of these tests were to determine if explosively generated rf signals exist and to determine polarization characteristics and the correlation between the signals. The presence of EM radiation was determined on the 90-MHz channel, since the intensity decreased porportional to the inverse of the distance from the source to the receiving antenna.

The polarization was concluded to be uniformly distributed, since two antennas at right angles to each other received about the same signals.

His maximum signals, on the order of 4×10^{-4} V/m, were obtained on the 6- and 90-MHz bandwidth channels. This is as close as he comes to providing the frequencies of the radiated signals.

In all cases, a visible light pulse was obtained before detection of the rf, which was delayed 80 to 160 μs from initiation of the explosion.

Takakura attributes the cause of the radiation to be ionization at the shock front produced by the explosion with the resulting production of dipoles and the acceleration of the resulting dipoles. In an appendix, he estimates the second time derivative of the average dipole moment to be 1.6×10^3 C m/s^2 and the average acceleration of the charge forming the dipole to be 10^9 m/s^2.

2.3 Kelly

Kelly [6] offers an overview of explosives, the resulting EM pulses, and the propagation characteristics of the pulses and sensing methods useful for detection. Kelly does not provide his own experimental results but discusses the results of previous investigators. He suggests that a unique signature for a given charge may not exist because of the dependence of output pulse on the method of initiation. It is expected that the faster the initiation, the higher the frequency components, since one would expect higher frequencies from fast rise time events and lower frequencies from slower rise time events.

He also discusses the effect of the wavelength of radiation on the dependence of the *E*-field on the distance from the source to the observer, which is summarized in the appendix of this report.

2.4 Stuart

In a classified Advanced Research Projects Agency (ARPA) report on Hostile Weapons Location Systems (HOWLS) [3], a summary of rf measurements from various weapons firings is presented. The most promising results were those from a Navy study by Lockheed in 1968. Frequencies were recorded in the 250-MHz to 1-GHz range for various caliber weapons. The ARPA report also includes a good summary of experimental results of the measurement of signals produced by three different types of explosives. This is a good starting point in trying to explain the mechanisms causing radiation from weapons. The equipment and experimental techniques are described in the report. With today's improved sensitivity and bandwidth, we should be able to duplicate and improve these observations.

Stuart also provided a literature review, most of which is unclassified. He found that the Soviets had been interested in rf from explosions and had done much basic work. They studied unconfined explosives and found that the rf energy is related to "the expansion of the gaseous products of detonation and can be explained on the basis of the kinetic molecular theory of gases by the nature of motion of the ionized particles in the pressure field." They also found that there is a characteristic signature from different kinds of industrial explosives that is determined mainly by the following:

- "the presence in the explosive composition of easily ionized additives, such as salts of alkali metals,

- the presence in the explosive composition of combustible additives, such as sawdust and aluminum, and
- various factors, such as the presence of casings, preventing the free escape and expansion of the explosion products. The polarity of the pulses is said to be determined by the change of the dipole moment with time."

The signatures of several different explosive compounds are shown in figure 3.

2.5 Gorshunov, Kononenko, and Sirotinin

Gorshunov, Kononenko, and Sirotinin [7] are Soviet investigators who investigated spheres and cylinders weighing from 1 to 5 kg and cast from a 50/50 "trinitrotolul hexogen" [sic] alloy. They investigated "the effect on the EM signal of different initiation methods, suspension height, mass and shape of the explosive charge, and external electric and magnetic fields." Instrumentation in the 30-Hz to 2-MHz range was used. They

Figure 3. Electro-magnetic pulses from detonation of various explosives.

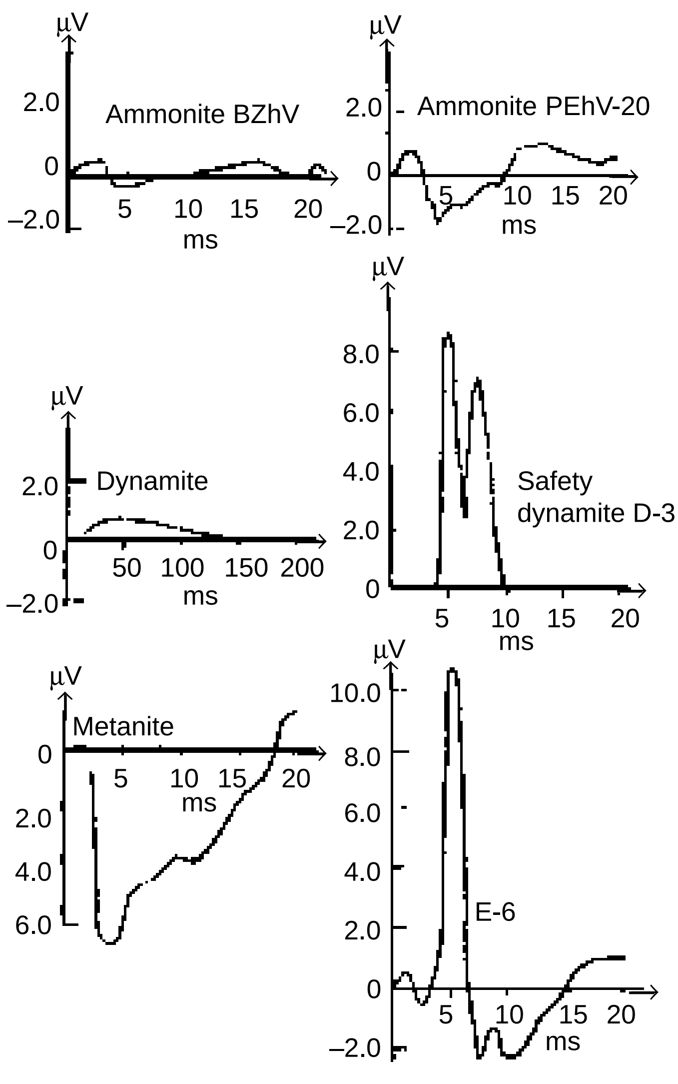

found that the time interval t_m between initiation of the detonation and the EM signal maximum depends on the cube root of the mass M of the explosive charge by

$$t_m = KM^{1/3} \quad , \tag{12}$$

where $K = 0.7$.

They also found that initiation by flame produced different signals than initiation by electrical pulse. Also, the electrical initiation of a horizontally mounted cylindrical charge initiated at one end produced signals of opposite polarity on antennas positioned on opposite sides of a plane perpendicular to the axis at its center. Reversing the direction of initiation reversed the polarity of the antennas.

For flame-initiated signals, electric fields up to 1000 V/m and magnetic fields up to 5 Oe in the explosion region had no effect on the signals. The signals do not depend on the suspension height of the explosive charge above the ground.

They believe that the EM signals are generated by electrical charges or currents that arise from electrified explosion products and that the asymmetry of the explosion is the "governing factor" in generating the signals. For electrically detonated explosives, the leads introduce the asymmetry, and for flame-initiated explosives, the geometry of the explosive charge determines the asymmetry.

2.6 Nanevicz and Tanner

Nanevicz and Tanner [8] attempted to reduce the rf noise on the order of 1 MHz that is generated on aircraft by triboelectric charging, a mechanism also discussed by Trinks [1], (sect. 2.1), as applied to projectiles. A footnote found in Nanevicz and Tanner's paper defines triboelectric charging:

> "Triboelectric charging occurs whenever two dissimilar materials are placed in contact and then separated. In the case of an aircraft flying through precipitation containing ice crystals, the ice crystals generally acquire a positive charge, leaving the aircraft with a negative charge."

When the charge builds up to a sufficiently high potential, it discharges via a corona discharge mechanism and produces rf noise in the 1-MHz band and interferes with radio reception aboard the aircraft (fig. 4). When various decoupling devices such as insulated conductors that are attached to the wing trailing edges are used, the intensity of *E*-fields on the aircraft is reduced, thus reducing the amplitude of rf static from the corona discharge (fig. 5).

Figure 4. Illustration of noise-coupling theorem.

[Reprinted with permission (see ref 8)]

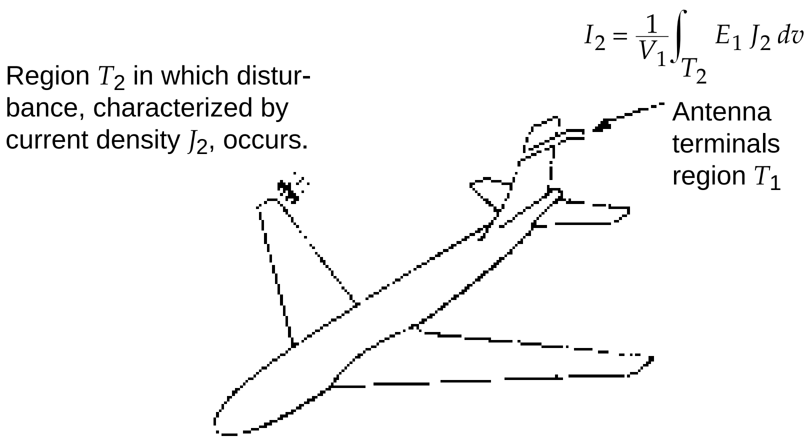

Situation 1: Voltage V_1 is applied to terminals T_1 producing field E_1 at all points of space and in particular in the region T_2.

Situation 2: Disturbance occurs in the region T_2 current; density J_2 is therefore finite in T_2. In response to the discharge, a current I_2 flows in the short-circuited antenna terminals T_1.

Figure 5. (a) *E*-field configuration at trailing edge of airfoil, (b) rf coupling field configuration around airfoil with isolated edge, and (c) static field configuration around flush decoupled discharger.

[Reprinted with permission (see ref 8)]

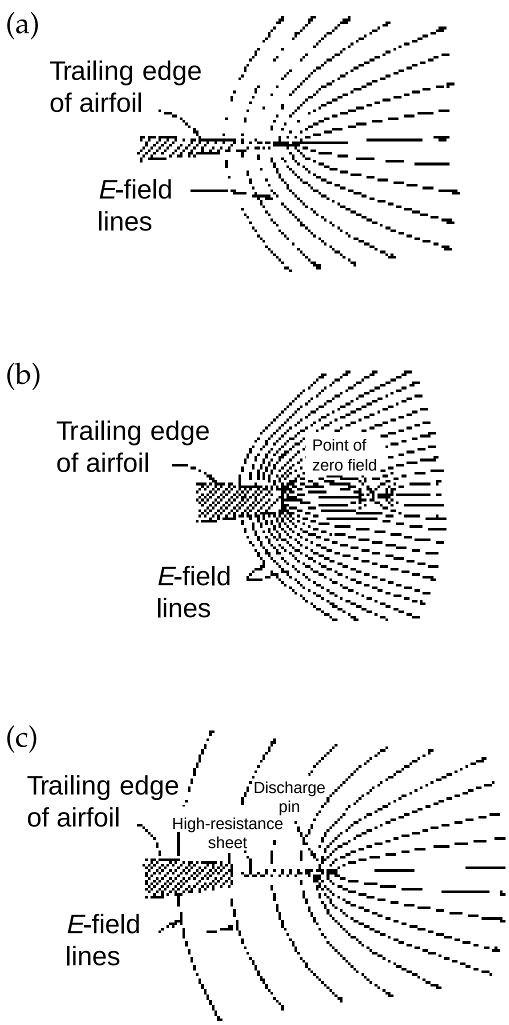

The corona rf is discussed only qualitatively in the report. A book by Leonard Loeb [9] discusses corona discharge in detail and should provide a basis for a quantitative understanding of this mechanism of rf generation. The corona effect will not be discussed further in this initial literature review, because it is not an explosive process, even though it is a possible source of radiation from projectiles in flight.

2.7 Curtis

Curtis [4] measured extremely low-frequency (ELF) signals from small (10 g) explosive charges, suspended 1 ft above the ground, and similar charges 1 ft under water. For the air tests, the receiving antennas were either stretched a few feet in the air normal to the direction of the charge or laid on the ground in the same position at a distance of 10 ft. The orientation made no difference in the measurements. For the water tests, a ferrite loop antenna was used at the bottom of the site, typically 8 ft away. The instrumentation filtered out all frequencies above 350 Hz. The signals in air exhibited the following features: they were delayed about 2 s from initiation of the explosive to the start of the major signal, they had a minimum frequency of 0.5 Hz, and they lasted 15 to 19 s (fig. 6). The signal amplitude observed at 10 ft was 0.5 mV/m. For the water tests, the signal lasted 2 s and the delay after initiation was 2 s, with a minimum frequency of 1 Hz. Audio frequency analysis showed that “the signals were distributed through the spectrum covered by the equipment, as expected.” The receiving antennas were not in the radiation zone; but in the static zone so the discussion of the ELF signals detected as “radiating fields” is a bit misleading. Curtis offered no theoretical explanation for the effects observed. Table 3 is a compilation of Curtis’s results that are provided in his report.

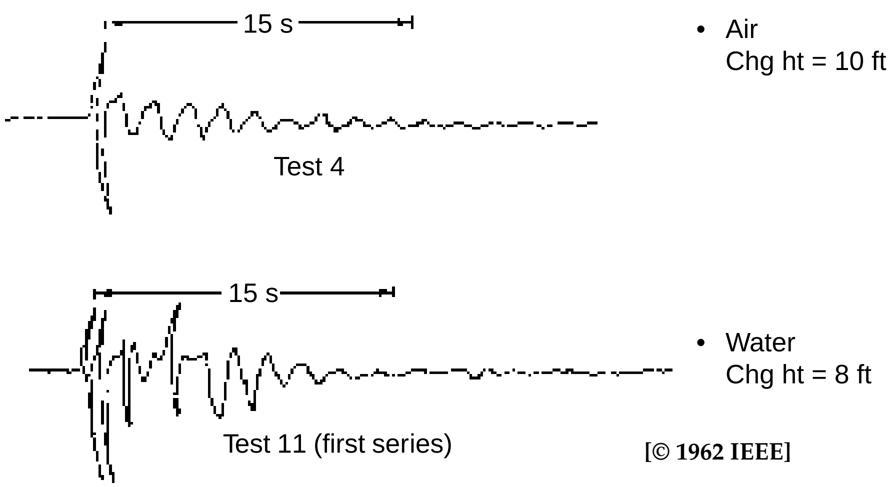

Figure 6. Low frequency rf from 10 g explosive charge.

Table 3. Results of Curtis's voltage measurements from detonating 10 g of RDX in air.*

Bandwidth of instrumentation channel	Antenna length	Distance from explosion	Signal duration	Range of calculated *E*-fields
1–350 Hz, 0.5 Hz minimum freq observed	20 ft (610 cm)	10 ft (305 cm)	19 s	5×10^{-4} V/m

*Curtis also made measurements of detonation of explosives submerged in 1 ft of water, but these were not included here, because the subject of this investigation is confined to detonations in air.

2.8 Cook

Cook [10] detonated 2- to 3-lb explosive charges 75 m above the ground with two antennas (he does not mention the type or length used) placed at 100 ft from the charge and located at right angles to each other. The peak signal recorded from each antenna was 200 mV, with an initial pulse frequency of about 5 kHz, using a cathode follower configuration with a cutoff frequency around 30 kHz. There is no mention of any gain characteristics of this setup, so that the field strength cannot be assessed. The resulting traces are shown in figure 7. In figure 7 (a), the traces recorded from each antenna have the same pulse shape for the first 150 μs, showing that the signal is not uniquely polarized. This agrees with the results by Takakura mentioned previously. Figure 7 (b) was a repeat of the test; however, the pulse shape was repeatable only for the first 150 μs. This demonstrates the difficulty many experimenters have had in repeating their results even under seemingly identical conditions.

Cook also measured explosive charges of various weights from 70 to 1100 g. Peak signals occurred when the charges were fired at heights equal to the radius of the expanded hot gas cloud. He reports that the

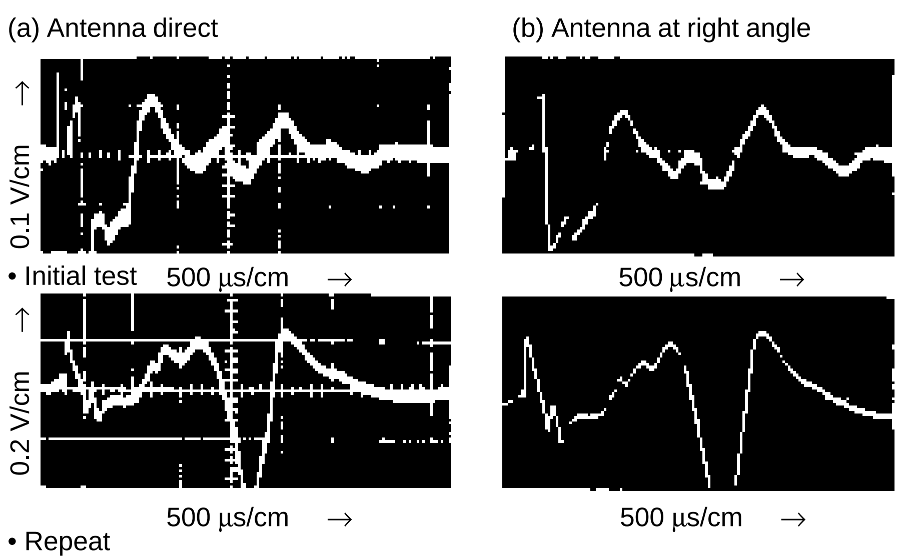

Figure 7. Rf pulse at 100 ft from detonation of 2 to 3 lb of composition B explosive mounted 30 in. above ground.

[Reprinted with permission (see ref 10)]

signal amplitude in an antenna at 30 ft (914 cm) from a charge suspended at a 90-cm height increases porportional to the 0.8 power of the charge mass. The measured signals for these tests were proportional to the inverse square of the distance from the source to the antenna, which is characteristic of an electrical field in the induction zone, even though the observation points are much closer (well within the static zone).

The frequency of the first quasi-sinusoidal portion of the pulse varied from 6.2 to 2.8 kHz, as the mass of the explosive was increased from 70 to 1100 g. Thus the frequency depends on the inverse cube root of the charge mass [(2.8 kHz/6.2 kHz) = $(1100\ g/70\ g)^{-1/3}$]. This is the same dependence as the reciprocal of the time from initiation to detonation of the explosive, as mentioned by Stuart [3] (sect. 2.4). We therefore may suppose that the pulses observed by Cook are caused by some effect that occurs during the detonation process.

When the shots were fired directly on the ground, no EM signal was obtained. Also, a grounded wire screen 150 cm above the charge eliminated the signal, possibly suggesting that the generation of the EM signal was related to the acceleration of electrons from the explosive gases in the earth's vertical electric field, which is about 100 V/m.

Cook proposed the following physical description of the phenomenon that caused the EM signal to occur as a result of the explosion: "During the initial expansion into the atmosphere of the gaseous products of detonation, at the front of which is the observed plasma, the gas cloud becomes charged, evidently as a result of polarization of the plasma at the surface of the expanding gas cloud under the influence of the atmosphere's vertical potential gradient and/or electrokinetics. After this gas cloud accumulates sufficient charge in this way, it may then be discharged by making a direct contact with ground or through a suitable grounded probe. The electrical pulse begins to radiate at the instant the discharge commences, the wavelength of the radiated pulse being then roughly proportional to the diameter of the gas discharged and to the conductivity of the ground."

2.9 Wouters

Wouters [11] analyzed data from two foreign tests as well as his own test. The first was a Soviet test by members of the Dremin Laboratory to determine the local *E*-field generated by detonation of a 1.3-kg cylindrical charge. The second test was of a 500-ton hemispherical high-explosive (HE) surface detonation observed by a team from the United Kingdom.

In his efforts to derive the pulse shape and amplitude, Wouters adopted an atomic physics approach in which he attempted to account for the blast temperature and its effect on ionizing the ambient air and explosive products, the resulting plasma, and the concentration of electrons and ions as a function of temperature. He considered ionic attachment, recombination, mobilities and conductivities, and charge acquisition by burn products and debris. He also considered the effect of geometric parameters and hydrodynamic considerations on the time evolution of the explosion and fireball. The detail of the description of the experiments is not sufficient to allow comparison with the physical behavior that he presents.

He does show rf pulses from two detonations, but he does not give details about the observation distance, antenna used, and instrumentation system sufficient to determine the *E*-field. The first detonation is from 1.3 kg of a cylindrical explosive charge, figure 8. Using the cube root relationship from Stuart [3] and the explosive mass and resulting frequency from Cook [10], we find that the expected time scale of the rf is 2.8 kHz × (1.3 kg /1.1 kg)$^{-1/3}$ = 2.65 kHz, or 0.3 ms. The time duration of the first part of the pulse is about 0.4 ms. The second detonation is a huge explosive, 500-ton hemispherical HE charge, figure 9. Applying the Stuart/Cook calculation to this explosive, 4.54 × 10^5 kg, gives 2.8 kHz × (4.54 × 10^5 kg /1.1 kg)$^{-1/3}$ = 37.6 Hz, or 27 ms. The first part of the pulse is about 32 ms, which is the expected time scale.

2.10 van Lint

One of the more recent experiments reported in the literature is by V.A.J. van Lint [12] of Mission Research Corporation. Measurements were made for explosions ranging from 0.01 to 345 kg. Various antenna configurations were used to capture broadband LF, narrow-band VHF (very high frequency), and UHF (ultrahigh frequency) signals. Most measurements

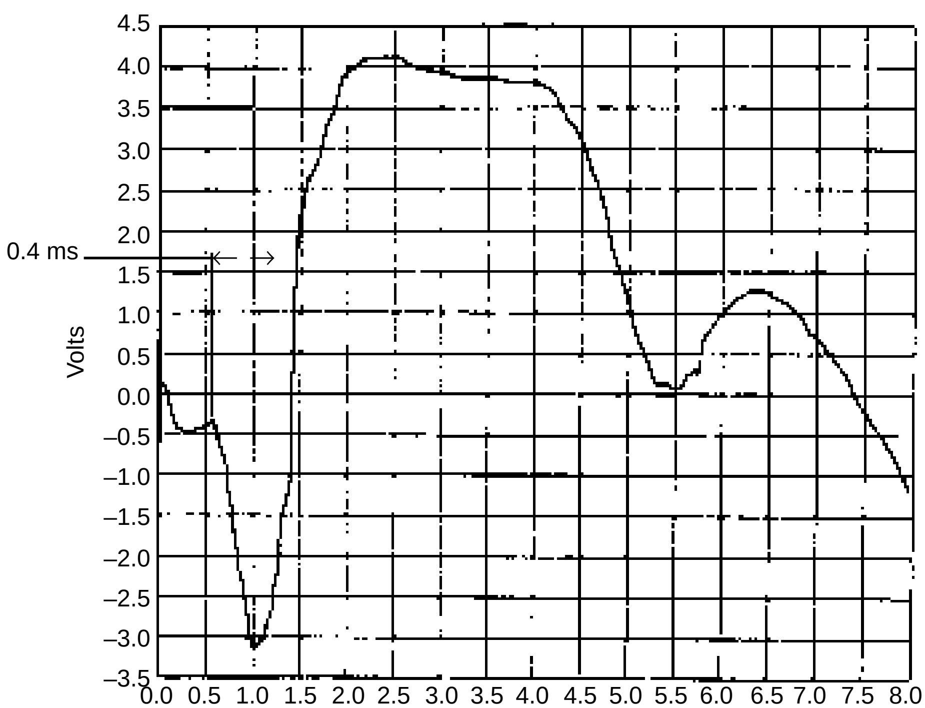

Figure 8. Typical trace from Soviet detonation of 1.3 kg of a cylindrical explosive charge.

[This illustration is a modification of an illustration appearing in a University of California Lawrence Livermore National Laboratory report authored by L. F. Wouters (see ref. 11). This report was prepared under the auspices of the Department of Energy.]

Figure 9. Rf trace from detonation of 500-ton hemispherical HE charge.

[This illustration is a modification of an illustration appearing in a University of California Lawrence Livermore National Laboratory report authored by L. F. Wouters (see ref. 11). This report was prepared under the auspices of the Department of Energy.]

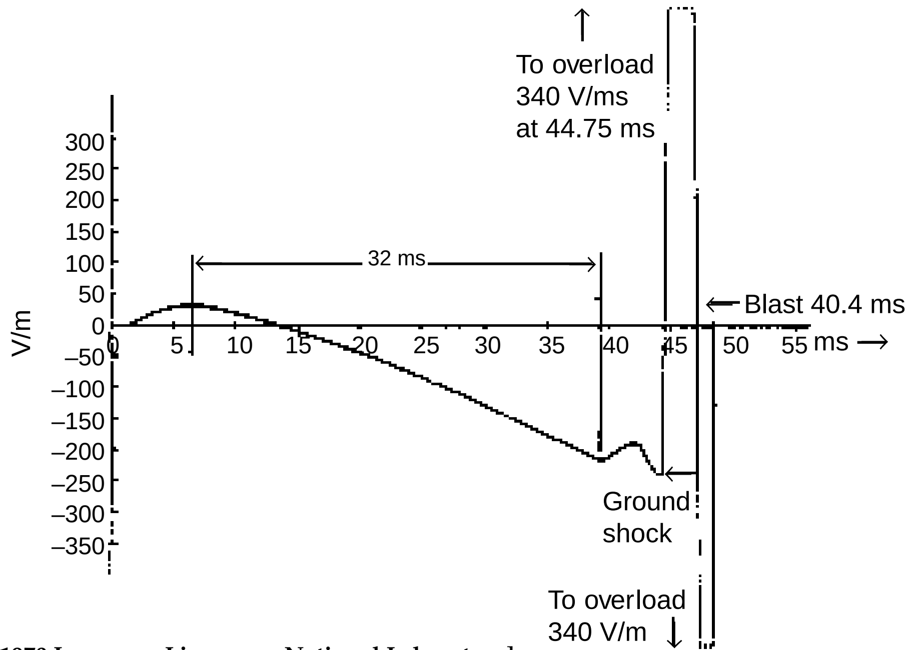

were performed either 140 or 200 m from the detonation, in the radiating zone for the higher frequencies. The results are presented graphically, but the discussion in the paper does little to draw conclusions on the group of measurements.

Van Lint proposed that most of the rf radiation is produced by electric sparks from detonation products and case fragments. Most of the rf bursts in these experiments occurred at 100 to 200 µs following detonation, after the case had fragmented, and while explosion particles were streaming through the spaces between fragments. Beyond this, van Lint proposed no further explanation for the measured signals.

2.11 Andersen and Long

Andersen and Long [13] showed that detonation of bare charges provided a distinctly different EM signature from detonation of encased charges. They suspended charges ranging in mass from 20 to 1087 g of tetryl or Composition B at a distance of 18 in. above a steel ground pad. Apparently, the charges were roughly cylindrical in shape and initiated from one end. The signals were received by two end-fed antennas, each connected to a cathode-follower circuit having an HF cutoff of 600 kHz. The output of each circuit was connected to a Tektronix 551 oscilloscope and recorded on a Polaroid camera. The antennas were positioned at various distances and angles from the charge axis. The oscilloscope sweep was initiated simultaneously with the initiation of the detonator. A time interval of 72 µs was required from initiation to completion of detonation. The EM signals were observed from 300 to 600 µs after the detonator was initiated.

2.11.1 *Effect of Casing*

Charges were encased with 0.5-in. thick plaster of Paris. The results are shown in figure 10 (a). The uncased signal amplitudes were small and unreproducible. The encased explosives produced a much higher signal. For example, a 2- × 4-in. cylindrical charge uncased had a barely distinguishable signal of 1 mV, as measured by an antenna at 4.27 m (14 ft) from the charge. With the casing, the signal increased to 18 mV with a pulsewidth of 6.5 ms. The 6.5-ms pulsewidth corresponds to a frequency band of 154 Hz, an LF signal. They also tested a “half-casing” configuration (fig. 10 (b)), which had a signal similar to the full-casing, but the signal amplitude was only 15 mV. The pulsewidth was about the same as the fully cased charge. The “half-casing” was defined as “full-casing applied to a lateral half of the charge only.”

2.11.2 *Effect of Seeding*

In another explosive configuration, the charges were seeded 15 percent by weight of sodium bicarbonate. It seems that the seeding was a mixture of the solid explosive with the sodium bicarbonate powder, but the text was not explicit. Andersen and Long also defined a “half-seeded explosive” as

Figure 10. Effect of casing and seeding on rf pulse from explosive charges.

[Reprinted with permission (see reference 13). Copyright 1965 American Institute of Physics]

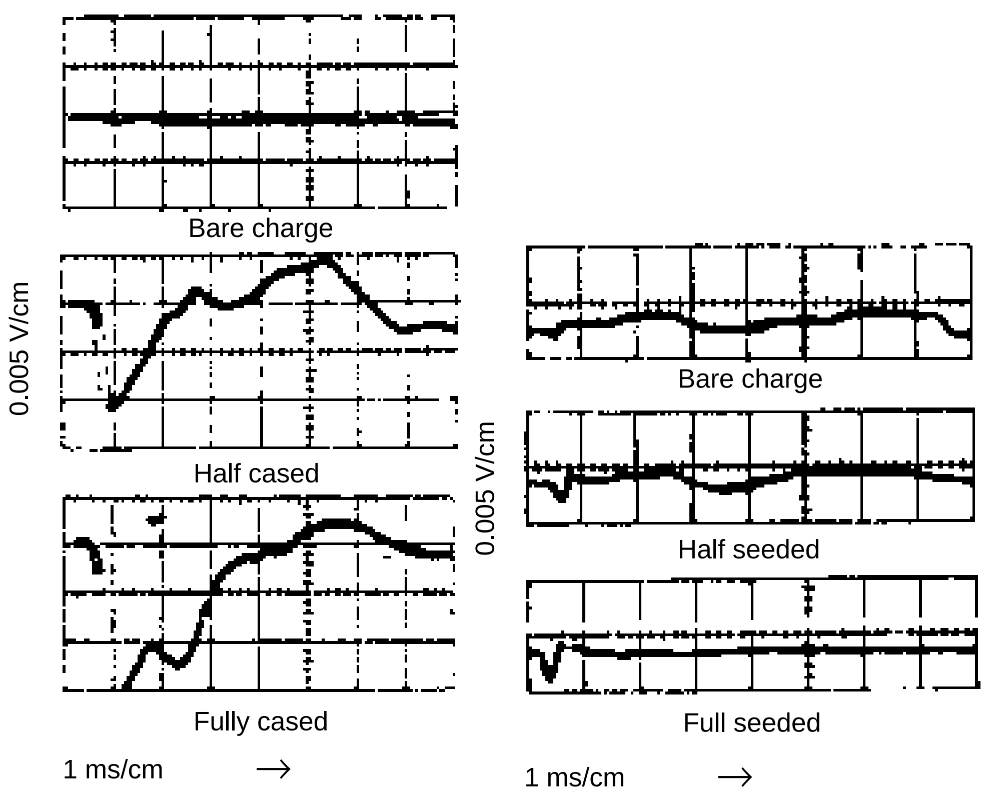

(a) Tetryl charges encased with 0.5-in.-thick plaster of Paris.

(b) Composition B charges seeded with 15 percent by weight of sodium bicarbonate.

“a full seeding applied to a lateral half of the charge only.” The antenna was at 4.27 m (14 ft) as in the casing experiment. The results are shown in figure 10 (b). The bare charge amplitude was about 2.5 mV and about 7 ms long. The full-seeded charge was about the same amplitude, but the pulse shape was suppressed, except for a 0.5-ms negative pulse at the beginning of the trace. The half-seeded explosive was similar to the full-seeded one, except that the pulse shape of the bare charge was not suppressed, but the negative 0.5-ms pulse at the beginning of the trace was almost the same amplitude as the full-seeded configuration. The 0.5-ms pulsewidth corresponds to a frequency band of 2 kHz, also an LF signal.

“The significant result obtained was that the much larger signal amplitudes of the cased and seeded charges correlated in a direct manner with the weight of the inert substance added to the charge. Thus, the average signal amplitudes of the half-seeded, fully-seeded, half-cased, and fully-cased charges stood in the ratio of 1.0, 2.6, 13.7, and 23.7, respectively, while the inert mass present in these charges was in the ratio of 1.0, 2.0, 10.6, and 21.3. This result shows that the dominant ion source producing the EM radiation from these charges was electrically charged particles of the pulverized casing material and the seeding agent ….”

2.11.3 Source of High-Frequency Radiation

Andersen and Long also detected HF signals between 400 and 500 MHz on detonating a 1.25-lb block of Composition C-4 suspended 0.91 m (3 ft) above the ground. Short random bursts were observed. They were attributed to collisions of charged solid particles of unequal potentials with each other or with the ground.

2.11.4 Conclusions From Andersen and Long

The work of Andersen and Long showed that the inert materials are a significant contribution to the radiated signal. They attributed the EM signal to the discharge of electrically charged solid particles that receive their charges by friction as they accelerate past electrically charged detonation products. The casing of conventional explosives would be metal, such as iron or steel, rather than the inert materials discussed in section 2.11.2 and probably would produce still different signals. They felt that the fragmentation properties of the casings therefore would affect the radiation significantly.

Their conclusions point to the source of radiation being ionized particles that arise during the detonation process with charges that appear initially on the detonation products. Subsequently, these charges are transferred by friction to the inert casing particles and fragments as they accelerate relative to the detonation products. Both low frequencies 150 Hz to 2 kHz and high frequencies 400 to 500 MHz were observed.

2.12 Adushkin and Solov'ev

Adushkin and Solov'ev [14] investigated an electric field pulse induced in the soil when an explosive charge was detonated underground. The source of charges that generate the *E*-field is similar to the source of charges that produce rf from detonations that occur aboveground, as in the papers reviewed above.

While estimating the charge buildup in the soil, they take into account the relaxation process within the plasma formed during the explosion. This includes an estimate of a time of 10^{-8} to 10^{-9} s for capture of the free electrons in the detonation products by oxygen molecules. They also provide, but do not derive, a formula for the relaxation of the ion charges because of the conductivity of the "weakly ionized gas." They also provide a formula for the time for the velocity distribution of particles—the text was not clear whether it was the ions or the electrons—in the plasma to become Maxwellian, which they estimate as 10^{-11} s.

They also provide a formula to estimate the charge captured by the "scattered medium," probably the soil, as a result of the detonation force, in terms of the volume of the soil that is interacting with "the ionized detonation products."

The analysis, while difficult to follow because of the omission of derivations of formulae, provides a starting point for a more thorough study.

This report refers to several other reports in Russian, which are included in a bibliography. The Russians therefore have much interest in rf from detonation of conventional explosives.

2.13 Fine and Vinci

Fine and Vinci [15], after conducting a review of the literature, developed a simple model of the thermal effects of the detonation, which they consider to be the largest source of EM radiation. The model involves several simplifying assumptions but is a first step at calculating frequency band, signal strength, and detection thresholds, as in section 3. The frequency bands and signal amplitudes predicted at a distance of 10 km for a mortar-sized projectile detonation are shown in table 4.

2.13.1 Description of Model

The calculation model is based on the assumption that the energy of detonation of the explosive material goes into the production of an outwardly traveling spherical shock wave. The temperature within the spherical region is extremely high, because of the addition of the heat from the explosion. Collisions between molecules, which are more frequent at high temperatures, cause ionization of molecules and production

Table 4. Calculation results for frequency bands and signal amplitudes 10 km from mortar-sized explosive detonation.

Radiation source	Charged particle	Conditions (1.5 ms) Frequency band	E-field (V/m)	B-field (G)*
Acceleration across shock front	O_2 ion	12 GHz	1×10^{-7}	4×10^{-12}
	N_2 ion	13 GHz	1×10^{-7}	4×10^{-12}
	Electron	2 THz	4×10^{-3}	1×10^{-7}
Acceleration across plasma shell	O_2 ion	18 kHz	4×10^{-10}	1×10^{-14}
	N_2 ion	20 kHz	5×10^{-10}	2×10^{-14}
	Electron	3 MHz	1×10^{-5}	5×10^{-10}
		Frequency†		
Acceleration in earth's magnetic field	O_2 ion	50 Hz	—	—
	N_2 ion	50 Hz	—	—
	Electron	3 MHz	—	—

* = B(weber/m^2) × 10^4
†The figures in this column are corrections to the printed symposium proceedings.

of free electrons.* The authors have considered three scenarios (fig. 11) for the production of radiation that they believe result from the acceleration of charged particles. The first two provide different-sized regions in which the charged particle acceleration occurs.

2.13.2 *Frequency Bands and Signal Levels*

In the first scenario (fig. 11 (a)), the expanding shock wave engulfs more atmospheric air at ambient temperatures (low velocities) and ionizes the air it passes through and accelerates the molecules to the higher velocities in the spherical region (fig. 12). The authors assume that the ionization and subsequent acceleration of the charged particles (ions and electrons) occur over the thin region of the shock front, which is on the order of 10^{-8} m. The frequency band that is calculated in this scenario is the reciprocal of the average travel time of a charged particle over that region. The acceleration of the charged particles produces radiation in the rf regime. This produces very high frequencies in the rf regime: 0 to 13 GHz for the positive ions and 0 to 2 THz for the electrons. The electron frequencies are too high to be detected by rf equipment in non-line-of-sight scenarios. The E-field amplitudes are 10^{-7} V/m for the positive charges and are much higher, 4×10^{-3} V/m, for the electron.

In the second scenario (fig. 11 (b)), the authors assume that the ionization and subsequent acceleration occur in a wider plasma region between the spherical shock front and a detonation wave that travels at a fraction of 0.75 of the speed of the shock front. The longer time for the electrons to

*At lower temperatures, the collisions also may induce vibration and rotational modes in the molecules, and at higher temperatures, the collisions may totally ionize the molecules. However, the authors ignored these additional phenomena in the analysis.

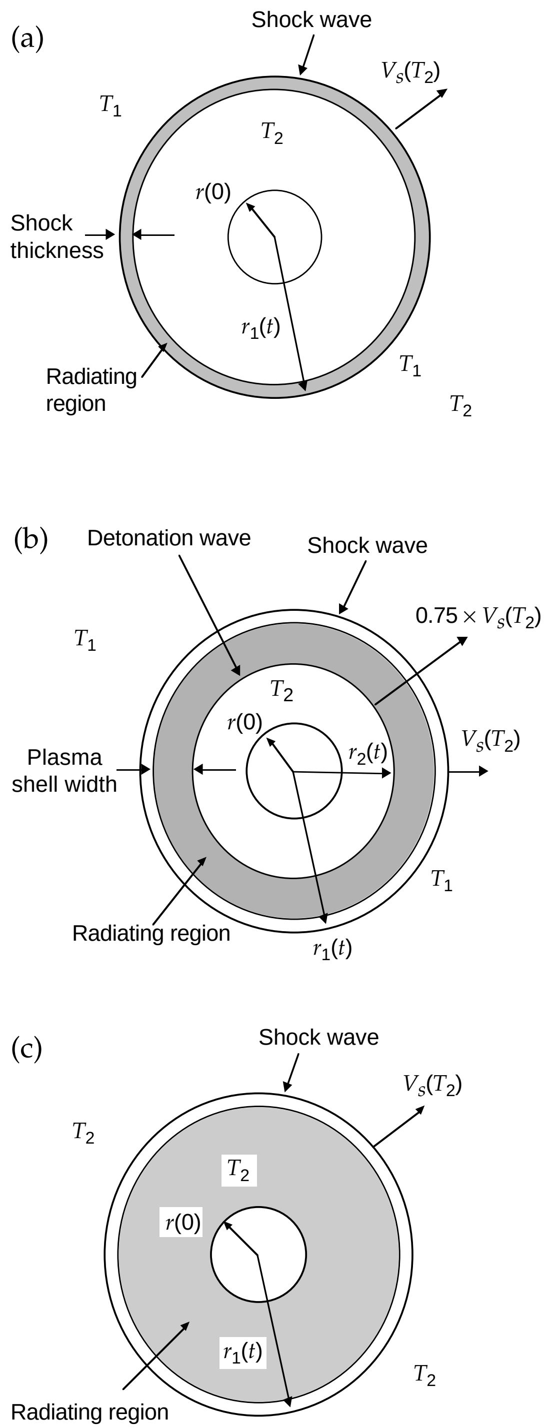

Figure 11. Three scenarios for production of rf radiation for a bare (uncased) explosive.

traverse the plasma region produces much lower frequencies in the rf region: 0 to 20 kHz for the positive ions and 0 to 3 MHz for the electrons. The frequency band that is calculated in this scenario is the reciprocal of the average travel time of a charged particle over that region. The *E*-field amplitudes are 4 to 5×10^{-10} V/m for the positive oxygen and nitrogen ions and 10^{-5} V/m for the electron (table 4).

Figure 12. Change in mean speed of charged particle caused by temperature rise across shock wave.

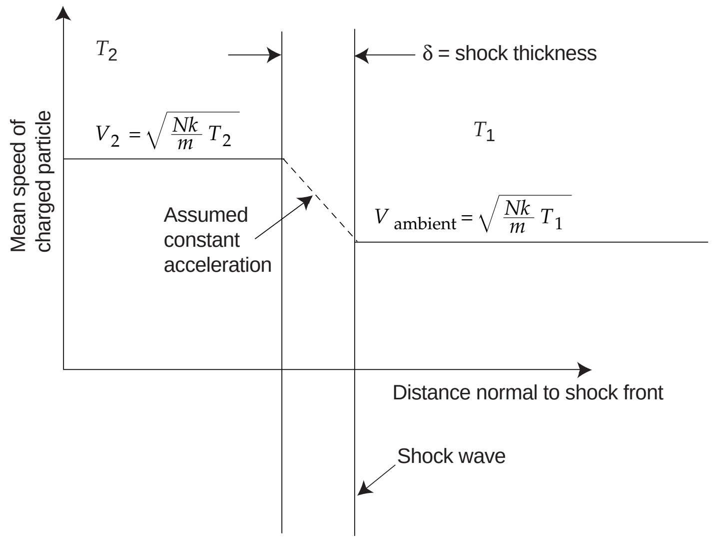

In a third scenario (fig. 11 (c)), the charged particles that already have been accelerated on passage through the shock front or plasma region are moving inside the spherical region with a high velocity corresponding to the high temperature within the region. The motion of these high-velocity charged particles in the earth's magnetic field of 0.3 to 0.7 G produces a radial acceleration that causes a well-defined frequency of radiation rather than a frequency band: 50 Hz for the positive oxygen and nitrogen ions and 3 MHz for the electrons. Note that this is within the 0- to 3-MHz frequency band from the second scenario, the particles' acceleration in the plasma region. The field values for this scenario were not included in the paper.

As shown in table 4, each scenario produces different frequency bands of radiation and signal levels. The most detectable particles from table 4 are the electrons, which (because of the lower mass in comparison with the oxygen and nitrogen ions) attain higher velocities and accelerations.

The model is modular so that it can be extended to account for other factors not yet incorporated, such as energy of bomb and projectile fragments, tube-launched projectiles, the ion species and concentrations, ionization and recombination rates, levels and relaxation times, and directional distribution of radiated energy per charged particle. Also, the effect of forming dipoles instead of free ions and electrons, as mentioned by Kelly [6] and Takakura [2], could be considered.

2.13.3 *Effect of Ion Concentration on* E-*Field*

Equation (21) from Fine and Vinci's paper gives the *E*-field in terms of the number of radiating particles as

$$E = \frac{1}{r}\sqrt{\frac{nAP\mu_o c}{2\pi}}\ \text{(V/m)}\ , \qquad (12)$$

where r is the distance in meters from the explosive to the observation point; n is the number of moles of radiating particles; A is Avogadro's number of particles per mole, 6.02×10^{23}; P is the radiated power in watts per particle; μ_o is the permeability of air taken equal to the permeability of free space, 1.26 μH/m; and c is the speed of light in air taken equal to the speed of light in empty space, 3.00×10^8 m/s. The quantity

$$N = nA \tag{13}$$

is the number of radiating particles. According to the above formula, the E-field is proportional to the square root of N. Thus if N decreases by a factor of 10^{-8}, then E decreases by a factor of 10^{-4}.

Equation (14) of the paper provides a formula to calculate the number of moles of an ideal gas in terms of its pressure and temperature:

$$n = \frac{pV}{RT} , \tag{14}$$

where p is the ambient pressure in N/m^2, V is the volume of gas in m^3, T is the temperature in Kelvins (K), and R is the ideal gas constant, 8.314 J/K-mole.

For ambient conditions of

$$p = 10^5\ N/m^2,\ V = 1000\ cm^3 = 10^{-3}\ m^3,\ T = 300\ K\ , \tag{15}$$

then

$$n = 4 \times 10^{-3}\ \text{moles}\ , \tag{16}$$

and

$$\begin{aligned} N &= 4 \times 10^{-3}\ \text{moles} \times 6.02 \times 10^{23}\ \text{particles/mole} \\ &= 2.4 \times 10^{19}\ \text{particles/mole}\ . \end{aligned} \tag{17}$$

These results will be used in the discussion, section 2.15, for comparing with Takakura's values.

2.14 Hull and Fine

Hull and Fine [16] applied Fine and Vinci's model [15] to investigate a shaped-charge detonation near a fuzed warhead to determine possible EM mechanisms that could disrupt the fuze circuit. The warhead was surrounded by detonation products of the shaped charge, rather than ambient air through which a shock wave passed. Therefore, the heat capacity of the detonation products and the thermal yield of the shaped charge established that the maximum temperature was from 2600 to 3600 K.

2.14.1 *Ionization Fraction*

The authors found two references (Hilsenrath and Klein [17] and Zel'dovich and Raizer [18]) that gave the ionization fraction of air as a function of temperature over two different temperature ranges. The two ranges are plotted in figure 13. The ionization rate in electrons/atom is plotted on a logarithmic scale versus temperature range from 1,000 to 500,000 K. Hilsenrath and Klein cover the lower portion from 1,500 to 15,000 K, which includes the range of interest in conventional explosives detonations of up to 5,000 K. Zel'dovich and Raizer cover the range of nuclear explosions from 20,000 to 500,000 K. Although the temperature ranges do not overlap, they seem to be approaching the same values in the range from 15,000 to 20,000 K, which suggests that they are branches of a single curve. Above 20,000 K, the atoms are multiply ionized, and above 200,000 K, they are fully ionized. In the range of conventional explosives temperatures, the atoms are at most singly ionized in extremely low concentrations. A temperature of 3,000 K, corresponding to the expected temperature of the penetration augmentation munition (PAM) shaped charge detonation, gives an ionization fraction of 10^{-8} electrons/atom, or more realistically, one electron removed per 100 million atoms. If the temperature drops to 2,000 K, a reduction of only 33 percent, the ionization fraction drops to 10^{-13}, a steep decline. Thus, the ionization fraction decreases sharply with decreasing temperature. The assumption was made that the ionization fraction of the detonation products, which include nitrogen, oxygen, and carbon monoxide ions, has the same temperature dependence as air and can be obtained from the figure. Therefore, the fraction of ionized detonation products of the PAM-shaped charge also should be 10^{-8} at 3,000 K.

Figure 13. ISS/rf modeling: air ionization fraction versus temperature.

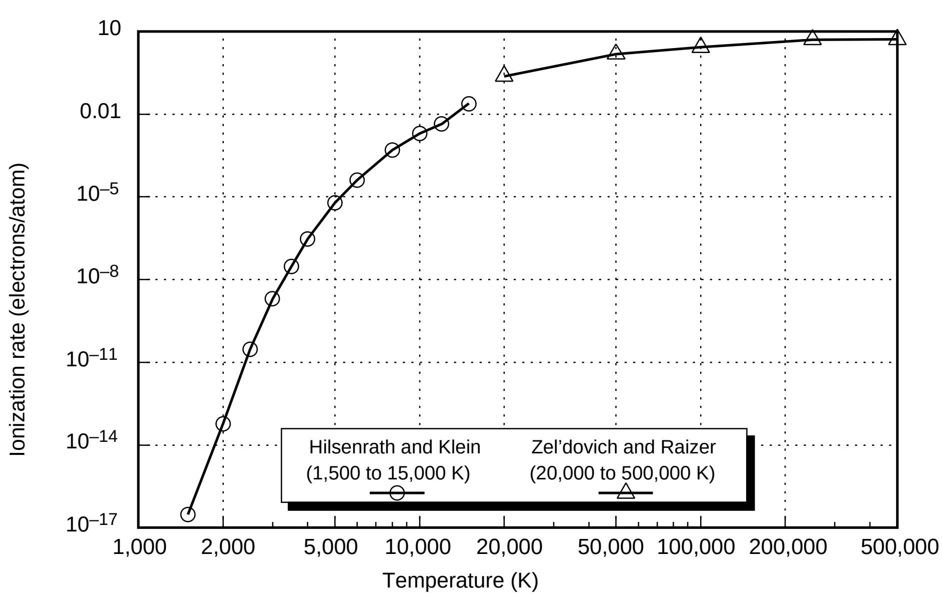

2.14.2 *Estimate of Shock Speed*

Knowledge of the shock speed permits one to estimate the time for the shock wave from a conventional explosion to hit the ground. Fine and Vinci [15] approximated the outward speed of a spherically expanding shock wave caused by an explosive detonation by using tabulated data in the shock tube literature [18] of shock speed versus temperature. Hull and Fine [16] show a curve of this relationship, (see fig. 14). The curve shows that for temperatures near the temperature of explosions, such as the PAM-shaped charge, assessed as 2,600 K, the shock speed is approximately 2200 m/s, or 2.2×10^5 cm/s.

Although the temperature, consequently the shock speed, diminishes as the shock wave spreads, we can use 2.2×10^5 cm/s as an average value to estimate the time delay. We do this in section 2.15.3.

2.15 Discussion of Results From Reviewed References

All the literature we surveyed includes the results of investigators who have observed radiation from detonation of explosives. Some of them have reported on signal levels, frequency bands, duration of the radiated pulse, and time delay from initiation of the explosive to detection of the rf pulse. They also have postulated possible causes of the radiation, some providing more detail than others. In this section, we intend to compare the results and possible causes.

2.15.1 E-*Field Signal Level*

Takakura [2] (sect. 2.2.2) reports E-fields on the order of 4×10^{-4} V/m in the frequency band from 6 to 90 MHz at distances on the order of 1 m from 0.1 to 0.4 g of lead azide. Curtis [4] (sect. 2.7) reported 5×10^{-4} V/m

Figure 14. Shock wave velocity versus temperature.

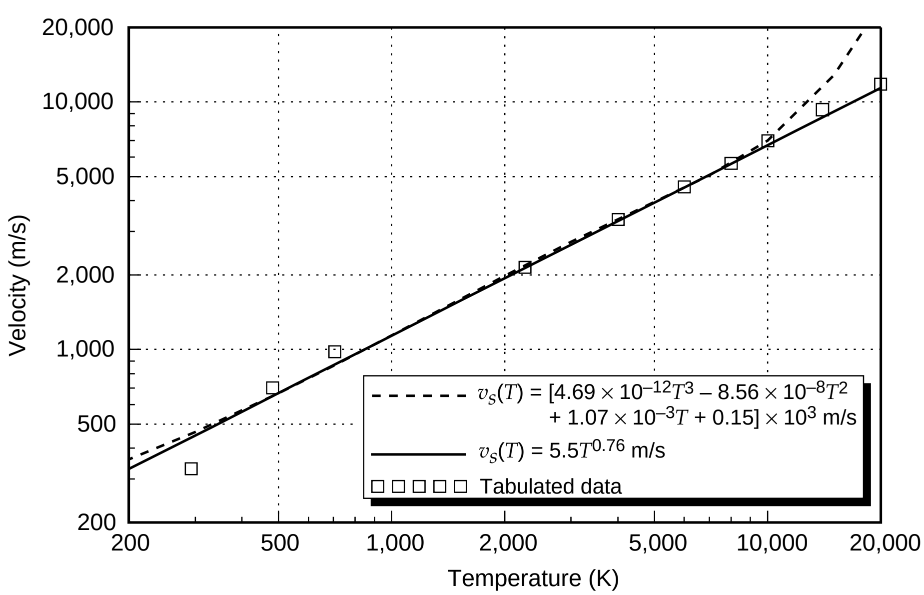

from 10 g of RDX (hexahydrotrinitro triazine) at a distance of 6.1 m in the frequency range up to 350 Hz, the cutoff frequency of his instrumentation. Curtis's results are roughly comparable to Takakura's if we assume that both explosives radiate the same, that is the *E*-field scales as the square root of the explosive mass (Fine and Vinci's model [15]) and inversely as the distance (radiated field). For example, if we take Takakura's signal of 4×10^{-4} V/m from 0.1 g at 1 m and extrapolate it by using the scaling laws to 10 g at 6.1 m, the result is 6.6×10^{-4} V/m. If we extrapolate the same signal from 0.4 g at 1 m to 10 g at 6.1 m, the result is 3.3×10^{-4} V/m. Both of these values are close to Curtis's cited value of 5×10^{-4} V/m at 6.1 m for 10 g.

We also might extrapolate Takakura's results to a mortar having about 1 lb (454 g) of explosives, so that we would expect an *E*-field of 1.3×10^{-6} V/m at 1 km, or 13×10^{-6} V/m at 100 m, or 13×10^{-4} V/m at 1 m. A bomb having 150 lb of explosive should produce an *E*-field of 16×10^{-6} V/m at 1 km, 160×10^{-6} V/m at 100 m, and 160×10^{-4} V/m at 1 m. These explosives and observation distances might be of interest in a field test to compare radiated fields from mortar and bomb detonations. (However, if the frequency is too low, this method might overestimate the field at the larger distances. See discussion in appendix.)

Fine and Vinci (sect. 2.13) calculated *E*-fields at 10 km for a mortar-sized explosive. Their scenario for electron acceleration behind a plasma region between a spherical shock wave and a blast wave traveling at 75 percent of the shock wave velocity predicts a frequency in the 3 MHz band. The calculated *E*-field gives an *E*-field at 10 km of 10^{-5} V/m assuming 100 percent of the molecules are singly ionized. Extrapolating this field to a distance of 1 m gives an *E*-field of 10^{-1} V/m at 1 m. The Fine and Vinci model provides that the *E*-field is proportional to the square root of the number of electrons radiating (sect. 2.13.3), so that an ionization fraction of 10^{-8} (Hull and Fine [16], sect. 2.14) reduces the *E*-field by 10^{-4} (sect. 2.13.3). Thus the *E*-field at 10 km would be 10^{-9} V/m, and at 1 m, it would be 10^{-5} V/m, or 0.1×10^{-4} V/m to compare with Takakura's result. Note that the scenario for the electron accelerating behind a shock wave would produce an *E*-field of 4×10^{-3} V/m at 10 km with 100 percent ionization and 4×10^{-7} V/m with 10^{-8} ionization. At 1 m with 10^{-8} ionization, the *E*-field would be 40×10^{-4} V/m, in comparison with Takakura. However, the predicted frequency is in the terahertz range, which is beyond the range of rf equipment and also is not amenable for detection out of the line of sight.

In summary, the *E*-fields observed by two independent investigators, Takakura and Curtis, are of the same level and are in the same levels as calculated by the Fine and Vinci model modified to account for the reduced degree of ionization expected from the Hull and Fine report. The Fine and Vinci model predicts the frequency band and signal level observed by Takakura. The signals observed by Curtis were much lower in frequency, even though he measured the same amplitude range.

2.15.2 *Frequency Bands*

The observations by different investigators cover a wide range of frequencies, as shown in table 5. The frequency bands calculated with the Fine and Vinci model are shown in table 4. The band of 0 to 13 GHz and 0 to 20 kHz includes radiation by accelerating positive ions. Accelerating electrons should produce 0 to 3 MHz in two of the scenarios calculated, 0 to 2 THz in the third scenario. Positive ions accelerating in the earth's magnetic field should radiate in the LF range 0 to 50 Hz.

Table 5 shows that all the observations covered a wide range of frequencies, but most of the investigators restricted themselves to a limited portion of the frequency band. For example, Takakura and Curtis tested small samples, 10 g or less. However, Takakura measured in the 6- to 90-MHz regime, but not in the LF regime; Curtis measured very low frequency signals with instrumentation that had an HF cutoff of 350 Hz. He did not look at the HF end of the spectrum. In so doing, each investigator probably missed a significant portion of the phenomenon. Thus to obtain the maximum information about the fields, an investigator must look at a wide range of frequencies: either with wideband instrumentation or with a range of instrumentation provided by several channels, each of limited bandwidth, that together cover the required spectrum.

2.15.3 *Time Delay From Initiation of Detonation to Maximum of Radiated Pulse*

The literature discussed in this report mentions two delay times: one, according to Cook [10], is the time for the shock wave to reach the ground, and the other, according to Stuart [3] and to Andersen and Long [13], is the time for the explosive detonation to be completed.

We first estimate the time for the shock to reach the ground. Takakura (sect. 2.2) and Curtis (sect. 2.7) listed the height above the ground that they suspended their explosives, 10 and 30 cm, respectively. Cook (sect. 2.8) wrote that the rf pulse should begin when the shock wave hits the ground and the charged particles behind it begin to discharge into the ground. The shock speed of 2.2×10^5 cm/s, as estimated by Hull and Fine [16] (sect. 2.14), enables this delay time to be estimated by dividing the above distances (10 and 30 cm) by this speed. Thus for 10 cm, the time delay is 10 cm/2.2×10^5 cm/s = 45 µs, compared with 80 to 160 µs observed by Takakura. For Curtis's 30 cm, the delay is 30 cm/2.2×10^5 cm/s = 136 µs. He reported a delay of 2 s, far larger than estimated with this method. Because his time response was limited to below 350 Hz, Curtis's instrumentation probably would not have allowed him to detect a 136-µs delay. We therefore see that the estimated shock velocity provides delay times on the order observed by Takakura, according to Cook's hypothesis.

Table 5. Frequency bands observed by investigators reviewed.

Investigator	Type of explosive used	Amount of explosive used	Delay/ duration of observed signals	Frequency range	Possible cause suggested by authors
		Experimental values of frequency ranges			
Trinks	Tube-launched artillery projectiles	None given	—	1–100 kHz 2 MHz–1 GHz 10 MHz–2 GHz	Muzzle flash, ionization of gases near muzzle. Pulses upon impact at target. Radiation at detonation from "microsparks" caused by charge equalization at detonation.
Takakura	Lead azide	0.1–0.4 g	80–100 µs delay	6–90 MHz	Acceleration of electrons ejected by ionization and dipole formation at shock front.
Stuart	Large caliber guns		—	250 MHz–1 GHz	None given, experimental results only.
Curtis	RDX	10 g	2 s delay/19 s duration	0.5–350 Hz	None given, experimental results only.
Gorshunov et al	50/50 trinitrotolul hexogen	1000–5000 g	—	30 Hz–20 MHz	Electrical charges generated asymmetrically from scattered electrified detonation products.
Cook	Composition B	70–1100 g	—	Below 10 kHz	Gaseous detonation products form a plasma at surface of gas cloud from ionization by passing through earth's electric field. Gas cloud discharges on contact with ground.
Wouters	None given	1,300 g 500 ton (= 4.5×10^8 g)	None explicitly given 8 ms duration (1.3 kg) 32 ms duration (500 ton)	—	Blast temperature ionizes detonation products and ambient air and produces a plasma.
van Lint	Bare spheres to metal-cased bombs	10–345,000 g (bare spheres to metal-encased bombs)	100–200 µs delay	50 MHz–1 GHz	Separation of charge at interface of explosion products and air to form a vertical dipole moment, with asymmetry induced by reflection of shock wave from ground. Electric sparks from explosion products interacting with casing fragments.
Andersen and Long	Bare, plaster-encased, and seeded explosives Tetryl, Composition B	20–1,087 g	300–600 µs delay	Less than 600 kHz	Detonation ionizes detonation products, which transfer charge by friction to inert casing particles and fragments.

(continued on next page)

Table 5. Frequency bands observed by investigators reviewed (cont'd).

Investigator	Type of explosive used	Amount of explosive used	Delay/ duration of observed signals	Frequency range	Possible cause suggested by authors
		Theoretical estimations of frequency ranges			
Fine and Vinci	Theoretical calculations on model of bare generic explosive with 25-MJ yield	Approximate size of 60-mm mortar	—	0–2 THz	Electrons accelerating across shock wave.
				0–3 MHz	Electrons accelerating across plasma shell.
				3 MHz	Electrons accelerating in earth's ambient magnetic field.

Many of the investigators noticed a delay from initiation of the detonation to the maximum of the electrical pulse. The delays are listed in table 6, along with the range of sizes of explosives tested. The time delays seem to be on the order of 100 to 600 μs regardless of the size of the explosive. The dependence on the cube root of the charge mass is well supported by the correlation between the observations of different investigators as discussed in section 2.15.1.

Andersen and Long report a delay time of 72 μs from a cylindrical charge length of 4 in. (10.16 cm). If the charge is initiated at one end, we divide this distance by the nominal detonation propagation speed of 10 mm/μs (= 0.1 cm/μs) to obtain a delay time of 102 μs, which is on the order of the time delays observed by Takakura and Cook.

This method of calculation is similar to the cube root dependence on explosive mass as proposed by Gorshunov et al [7]. If the explosive is a sphere initiated at its center, and a uniform detonation propagation rate is assumed, then the time from initiation to completion of detonation is proportional to the radius, which is proportional to the cube root of volume, or its equivalent, the mass divided by the density.

2.15.4 *Fraction of Particles Radiating*

Takakura uses a value of 10^{10} radiating particles per cm^3 to estimate the acceleration of a radiating dipole (sect. 2.2.3). It is useful to obtain a similar value from the Fine and Vinci model (sect. 2.13.3). At ambient conditions, the total number of particles per mole is 2.4×10^{19}. If the temperature is increased from 300 to 3000 K, corresponding to the approximate temperature of an explosive detonation such as PAM, then the figure will drop to 2.4×10^{18}, if we assume that 100 percent of the particles present are ionized and therefore radiating. If, as Hull and Fine report (sect. 2.14), the ionization fraction is only 10^{-8} (= 10^{-6} percent instead of 100 percent), then the result is 2.4×10^{10} radiating particles per cm^3, which is about the same value that Takakura used. It therefore appears that Takakura used an ionization fraction about equal to that determined by Hull and Fine.

Table 6. Time delay from initiation to beginning of pulse.

Investigator	Mass of explosives	Time delay from initiation to beginning of pulse
Takakura	0.1–0.4 g	80–160 µs
Gorshunov et al	1–5 kg	$t = kM^{1/3}$
Cook	70–1100 g	Time for charged particle gas cloud to expand and contact the ground. Wavelength of radiation is proportional to the gas cloud diameter when it contacts the ground.
van Lint	10–345,000 g	100–200 µs
Andersen and Long	20–1087 g, bare, cased, and seeded charges	300–600 µs (72 µs from initiation to detonation)

2.15.5 *Applicability to Conventional Weapons*

Most of the researchers reviewed in this report investigated bare, uncased explosives. Many common explosives that the military uses are mortar and artillery shells, grenades, and bombs that are made up of metal-encased explosives. The effect of casings, even though they were plaster of Paris, and not metal, was addressed by Andersen and Long. They found that the signal amplitudes were increased by at least a factor of 10. The presence of iron and steel casings on real munitions should have a similar effect on signals, increasing the observed *E*-fields beyond what has been estimated in this report.

The several possibilities expressed about factors that affect the rf pulse shape such as explosive size, shape, composition, and proximity to ground or other objects, suggest that further investigation of the dependence of the rf signal on explosive events could lead to the ability to identify weapons from their explosive rf signature.

3. Summary

Investigators have detected EM radiation from detonation of conventional explosives over the frequency range from 0.5 Hz to 2.0 GHz, as summarized in table 5. At least two observers have detected signals in the same frequency bands. In most cases, the detection distance has been within 200 m of the explosive event. This corresponds to the induction zone for frequencies below 300 MHz; hence, the magnitude of the radiated field has not been established.

The radiation is believed to be related to the production and separation of ionized particles and electrons caused by the heat of the explosion that generates a plasma. Some investigators feel that the radiation is caused by the acceleration of the charged particles themselves—either individually or as dipoles—and others believe that the radiation begins as a current pulse that is initiated when the charged particles in the plasma strike the earth, or other conducting material such as bomb casing fragments. Most investigators believe that the duration of the explosive event affects the radiation, since some have observed the main radiation pulse to occur from 60 to 200 μs after initiation of the explosion. This time corresponds approximately to the time required for the blast-generated shock wave traveling at supersonic speed to reach the ground (depending on proxim ity to the ground at initiation). However, when detonating small explosives, Curtis found a delay of 2 s, which is longer than any known conventional explosive event

A calculation model has been developed as a first step at calculatin frequency bands, signal strength, and detection thresholds. It addresse three mechanisms of radiation production and shows, as other observer have reported, that signals may be obtained from very low frequencies t very high frequencies and that radiation from the electron, rather tha positive ions, is most likely to be detected.

Acknowledgment

The authors acknowledge the help of David Hull for his suggestions on the content and organization of the first draft, Dr. Christian Fazi for reviewing the report, and Michael Kolodny for his constant encouragement throughout the project.

References

1. Trinks, H., “Electrical Charge and Radiation Effects Near Projectiles and Fragments,” Harry Diamond Laboratories, R-850-76-1, September 1976.

2. Takakura, Tatuo, “Radio Noise Radiated on the Detonation of Explosive,” Publications of the Astronomical Society of Japan, Vol. 7, No. 4, 1955, pp 210–220.

3. Stuart, William D., “Data Interpretation for Hostile Weapons Location Program, Vol. IV: Electromagnetic Emissions from Weapons and Explosions,” Advanced Research Projects Agency (now DARPA), ESD-TR-75-221, June 1975.

4. Curtis, George D., “ELF Electromagnetic Radiation From Small Explosive Charges in Air and Water,” Proceedings of the Institute of Radio Engineers (IRE), November 1962, pp 2298–2301.

5. ter Haseborg, J. L., and Trinks, H., “Electric Charging and Discharging Processes of Moving Projectiles,” IEEE Transactions on Aerospace and Electronic Systems. Vol. AES-16, No. 2, March 1980, pp 227–231.

6. Kelly, B., ”EMP From Chemical Explosions,“ Group P-14, Los Alamos National Laboratory, March 1993.

7. Gorshunov, L. M., Kononenko, G. F., and Sirotinin, E. I., “Electromagnetic Disturbances Accompanying Explosions,” Soviet Physics JEPT, Vol. 26, No. 3, March 1966, pp 500–502.

8. Nanevicz, J. E., and Tanner, R. L., “Some Techniques for the Elimination of Corona Discharge Noise in Aircraft Antennas,” Proceedings of the IEEE, January 1964, pp 53–64.

9. Loeb, Leonard, *Electrical Coronas: Their Basic Physical Mechanisms*, Berkeley, California, University of California Press, 1965.

10. Cook, Melvin A., *The Science of High Explosives*, New York, Reinhold Publishing Corporation, 1958, pp 159–171.

11. Wouters, L. F., “Implications of EMP From HE Detonation,” Symposium Proceedings, AFSWC Symposium, Albuquerque, New Mexico, 12–13 March 1979. UCRS-72149/Preprint Lawrence Radiation Laboratory, University of California, Livermore, 15 January 1970.

12. van Lint, V.A.J., ”Electromagnetic Emission From Chemical Explosions,“ IEEE Transactions on Nuclear Science, Vol. NS-29, No. 6, December 1982.

13. Andersen, W. H., and Long, C. L., “Electromagnetic Radiation From Detonating Solid Explosives,” J. Appl. Phys., Vol. 36, No. 4, April 1965, pp 1494–1495.

14. Adushkin, V. V., and Solov'ev, S. P., "Electrical Field Arising During Ejection Explosion," Moscow, translated from Fizika Goreniya i Vzryva, Vol. 26, No. 4, July–August 1990, pp 117–121.

15. Fine, Jonathan E., and Vinci, Stephen, "Causes of Electromagnetic Radiation From Conventional Explosives," 1997 Sensors and Electron Devices Symposium, University of Maryland, College Park, MD, 14–15 January 1997.

16. Hull, David M., and Fine, Jonathan E., "Possible Upset Mechanisms of the PAM FTC Fuze Related to Explosively Generated Electric Charges: A Preliminary Study," U.S. Army Research Laboratory Report, ARL-MR-373, Adelphi, MD, July 1997.

17. Hilsenrath, J., and Klein, M., "Tables of Thermodynamic Properties of Air in Chemical Equilibrium Including Second Viral Corrections From 1500 to 15,000 K," Arnold Engineering Development Center, Tullahoma, TN, AEDC-TR-65-68, March 1965.

18. Zel'dovich, Ya. B., and Raizer, Yu. P., *Physics of Shock Waves and High-Temperature Hydrodynamic Phenomena*, Vol. I, New York, Academic Press, 1967.

Bibliography

Boronin, A. P., Medvedev, Yu. A., and Stepanov, B. M., "Electrical Pulse From the Pulsations of a Volume of Explosion Products From a Charge of High Explosive," Soviet Physics-Doklady, Vol. 17, No. 9, March 1973, pp 925–928.

Boronin, A. P., Medvedev, Yu. A., and Stepanov, B. M., "Short-Wave Radio Emission and the Shock Wave From an Explosion," Soviet Physics-Doklady, Vol. 15, No. 4, November 1970, pp. 464–467, translated from Doklady Akademii Nauk SSSR, Vol. 192, No. 1, May 1970, pp 67–70. (Original article submitted 3 July 1969.)

Butterworth, Institute of Physics, Proceedings of the Conference on Electrostatics, Ser. No. 48, 1979.

Coffey, L. (BTI), "Operation Sailor Hat, EMP Investigation," POR-4059 (DASA).

Cook, M. A., Keyes, R. T., and Lee, L. D., "Measurements of Ionization and Electron Densities in the Detonation Wave of Solid Explosives," Technical Report No. 1, Contract AF-18(603)-100, ERG, University of Utah.

Danek, W. et al (Engrg Physics Co.), "Operation Distant Plain, Close-in Particle Velocity," DASA 2021.

Dawson, G. A., "Pressure Dependence of Waterdrop Corona Onset and Its Atmospheric Importance," J. Geophys. Res., Vol. 74(28), 1969, pp 6859–6868.

Dicke, R. H., "The Measurement of Thermal Radiation at Microwave Frequencies," Rev. Sci. Instrum., Vol. 17, 1946, pp 268–275.

Dickey, F. R., "The Production of Millimeter Waves by Spark Discharges," Technical Report 123, Cruft Laboratory, Harvard University, July 1951.

Frederick, B., August, G., and Nanevicz, J., "Corona Noise Investigation," Final Report, Contract DAAB07-86-C-H070, SRI Project 2559, 20 July 1987.

Gertsenshtein, M. E., and Sirotinin, E. I., "The Nature of the Electrical Impulse in an Explosion," translated from Zhurnal Prikladnoi Mekhyaniki i Tekhnicheskoi Fiziki, Vol. 11, No. 2, March–April 1970, pp 72–75.

Giori, K., August, J., and Swift, T., "Corona Noise Detection Experiments," SRI international final report, Project 2559, August 1990.

Gorshunov, L. M., et al, "EM Disturbances in Explosions," translated, U.S. Library of Congress, ARD Rpt 68–88.

Hayes, B., "The Detonation Electric Effect," J.A.P., Vol. 39, p 507.

Heirtzler, J. R., "The Longest Electromagnetic Waves," Scientific American, Vol. 206, March 1962, pp 1228–1237.

Hull, D., and Wrenn, M., "Helicopter Charge Measurements," Harry Diamond Laboratories, R-ST-SA-91-01, 20 June 1991.

Johansson, C. H., and Person, P. A., *Detonics of High Explosives,* New York, Academic Press, 1970.

Koch, B., "Emission of Short Electromagnetic Waves During Explosive Processes," LRSL, Technical Note 23a/50, 1950.

Kolsky, H., "E&M in Explosions," *Nature*, Vol. 173, 1954, p 77.

Langmuir and Tanis, "The Electrical Charging of Surfaces Produced by the Impact of High Velocity Solid Particles," General Electric Co., Schenectady, New York, Contract W-33-106-SC-65, May 1945.

Ma, M. T., "How High is the Level of Electromagnetic Fields Radiated by an ESD?" Proceedings of 8th Zurich EMC Symposium, March 1898, pp 361–366.

Malinovskii, A. E., *J. Chem. Phys.*, U.S.S.R., Vol. 21, 1924, p. 469.

Manuel, "Models With Two Exponential Functions for Comparing the Spectra of Lightning, Nuclear Radiation Sources and Electrostatic Discharge Sources," Administration for Material Supply of the Ministry of Defense, March 1981.

Martner, S. T., and Sparks, N. R., "The Electroseismic Effect," Geophysics, Vol. 24, April 1959, pp 297–308.

McKenna, P., Dalke, R., Perala, R., and Steffen, D., "Evaluation of the Observability/Detectability of Electrostatically Charged Rotorcraft," Contract N00019-88-C-0301, Electromagnetic Applications, Inc., Phase I Final Report EMA-89-R-36, March 1989.

Molmud, P., "Frictional Electricity in Missile Systems," American Rocket Society Journal, Vol. 29, January 1959, pp 73–74.

Pitts, Felix L., Perala, Rodney A., and Lee, Larry D., "New Results for Quantification of Lightning/Aircraft Electrodynamics," Electromagnetics, Vol. 7, 1987, pp 451–485.

Present, R. D., *Kinetic Theory of Gases*, New York, McGraw-Hill, Chapters 3, 8, and 11, 1965.

Radasky, W. A., "An Examination of the Adequacy of the Three Species Air Chemistry Treatment for the Prediction of Surface Burst EMP," DNA-3880T, December 1975.

Reif, F., *Fundamentals of Statistical and Thermal Physics*, New York, McGraw-Hill, Chapters 12, 13, and 14, 1965.

Reif, F., *Statistical Physics* (Berkeley Physics Course, Vol. 5), New York, McGraw-Hill Book Co., 1965, pp 248–249.

Roper, G. B. (UK/AWRE), "Operation Sailor Hat, EMP & VLF Measurements, etc," POR A4060 (DASA).

Rust, W. David, and Krehbiel, Paul R., "Microwave Radiometric Detection of Corona From Chaff Within Thunderstorms," Journal of Geophysical Research, Vol. 82, No. 27, 20 September 1977.

Savitt, J., “A Method for the Observation of the Ionization Profile Behind Explosive Produced Shocks in Air,” NAVORD 3589, 16 December 1953.

Schibuya, N., Koizumi, M., Takahashi, T., and Ito, K., “Radiation From the Coupling Plane of Indirect Electrostatic Discharge,” Faculty of Information Engineering, Takashaku University, 815-1 Tatewachi, Hachioji 193, Tokyo, Japan.

Sears, F. W., “An Introduction to Thermodynamics, the Kinetic Theory of Gases, and Statistical Mechanics,” 2nd ed., Reading, MA, Addison-Wesley, 1953, pp 256–258.

Stann, B. L., “An Air Target Electrostatic Fuze,” Harry Diamond Laboratories, HDL-TR-1977, March 1981.

Stann, Barry, and Sztankay, Greg, “Electrostatic Sensing for Tank Hit Avoidance,” White Paper to Andrus Niiler, AMSRL-WT-WD, 22 September 1993.

Tanner, R. L., “Radio Interference From Corona Discharges,” Stanford Research Inst., Menlo Park, CA, Technical Report 37, Contract AF 19(604)-266, SRI project 591, April 1953.

Tanner, R. L., and Nanevicz, J. E., “An Analysis of Corona-Generated Interference in Aircraft,“ Proceedings of the IEEE, Vol. 52, No. 1, January 1964, pp 53–64.

Tanner, R. L., and Nanevicz, J. E., “Precipitation Charging and Corona-Generated Interference in Aircraft,” Stanford Research Inst., Menlo Park, CA, Technical Report 73., SRI project 2494, Contract AF 19(604)-3458, April 1961.

Tanner, R. L., and Nanevicz, J. E., “Precipitation Generated Interference in Jet Aircraft,” 1959 IRE National Convention Record, pt. 8, pp 118–125.

ter Haseborg, J. L., and Trinks, H., “Electric Charging and Discharging Processes of Moving Projectiles,” IEEE, Vol. AES-16, No. 2, pp 227–232, March 1980.

Trinks, H., “Electromagnetic Radiation of Projectiles and Missiles During Free Flight, Impact, and Breakdown; Physical Effects; and Applications,“ presented at 4th International Symposium Ballistics, Monterey, CA, October 1978.

Trinks, H., and ter Haseborg, J. L., “Detection and Ranging of Electric Charged Helicopters,” 8th International Aerospace and Ground Conference on Lightning and Static Electricity, Fort Worth, TX, June 1983.

Trinks, H., and ter Haseborg, J. L., “Electric Field Detection and Ranging of Aircraft,” IEEE Transactions on Aerospace and Electric Systems.

Walker, C. W. (Lawrence Radiation Laboratory), “Observations of the Electromagnetic Signals From High Explosive Detonation,” Symposium Proceedings AFSWC Symposium, Albuquerque, NM, 12–13 March 1970.

Appendix. Observation Zones and Frequency

The types of experiments reported in the literature most often involved detonating an explosive charge and measuring the *E*-field at specified distances from the charge. It is important to establish from these measurements whether or not the fields measured correspond to a radiating source, because radiating fields are detectable far from the source and therefore are potentially more useful to military personnel at far off range in identifying and locating the sources of the radiation. Quasi-static, or nonradiating, fields are detectable only comparatively near the source. Of course, the far-zone definition will change with frequency detected, since the near zone of some LF signals may extend to a distance of several kilometers. Therefore detection of LF signals may be possible at these distances, even though the detection point is in the near zone.

Kelly* hypothesizes that an explosion causes a temporary separation of the charges that make up the neutral molecules of explosive products. The radiation is caused by the time-dependent separation and recombination of these charges. Each pair of charges, having equal and opposite polarity, forms a dipole. Therefore Kelly, Wouters,† and Kolsky‡ have identified the electric dipole as being a good approximation to the distribution of radiating charged particles produced by the explosion.

Kelly states that a time-dependent charge separation produces the pulse, with a time delay associated with the charge mass. This charge separation is caused by high temperatures in the explosive region. The work done in separating the charges is responsible for a large voltage difference capable of producing an electrical discharge. Therefore the pulse propagation can be modeled to a first order approximation by considering an electric dipole as the dominant source of the variations in the electric and magnetic fields generated by the separation of charges. This hypothesis leads to the following expressions for the electric and magnetic fields of an electric dipole that lies along the z-axis of a polar coordinate system, where the dimensions of the dipole are very small compared to λ, the wavelength of radiation ($= 2\pi/k$):

$$E_r = -\frac{pk^3}{2\pi\varepsilon}\cos\theta\left[\frac{j}{(kr)^2} - \frac{1}{(kr)^3}\right]\exp\left(j(kr - \omega t)\right) , \tag{A-1}$$

$$E_\theta = -\frac{pk^3}{4\pi\varepsilon}\sin\theta\left[\frac{1}{(kr)^3} - \frac{j}{(kr)^2} - \frac{1}{kr}\right]\exp\left(j(kr - \omega t)\right) , \tag{A-2}$$

---

*B. Kelly, "EMP From Chemical Explosions," Group P-14, Los Alamos National Laboratory, March 1993.

†L. F. Wouters, "Implications of EMP From HE Detonation," Symposium Proceedings, AFSWC Symposium, Albuquerque, New Mexico, 12–13 March 1979. UCRS-72149/Preprint Lawrence Radiation Laboratory, University of California, Livermore, 15 January 1970.

‡H. Kolsky, "Electromagnetic Waves Emitted on Detonation of Explosives," *Nature*, 9 January 1954, p. 77.

$$H_{\phi} = -\frac{\omega p k^2}{4\pi} \sin\,\theta \left[\frac{j}{(kr)^2} + \frac{1}{kr}\right] \exp\left(j(kr - \omega t)\right)\ , \qquad \text{(A-3)}$$

where $p = p(t)$ is the time-dependent dipole moment, $k = 2\pi/\lambda$ = wave number, and $\omega = 2\pi f$, where f is the frequency of radiation. Figure A-1 shows the coordinates and field lines.

Equation (A-1) shows a radial component, E_r, that approaches zero as r becomes quite large and increases as the cube of $1/r$ as r approaches zero. The first term in the brackets, the inverse square term in r, which has j as a coefficient, is known as the transition term. It does not contribute the radiated energy, but does contribute to the energy storage during oscillation.* The second term, because of the inverse cube dependence on r, is the static dipole field. These fields may be described in terms of three components—electrostatic, inductive, and radiating—according to the dominating term at a particular distance from the source. There is no radiation since the radial E-field approaches zero faster than $1/r$ as the observation distance becomes very large.

Equation (A-2), for the transverse E-field, has three terms. The first term, inverse cubic, is the static dipole term as mentioned in the previous paragraph. The second term, inverse square with j as a coefficient, is the transition term, which contributes only to the stored energy per cycle. The third term, inverse r, is the radiation term, which contributes to the radiated power.

Equation (A-3) shows that the transverse H-field, H_ϕ (which is the only component of the H-field), has a transition term and a radiation term. Far from the source, the field becomes transverse and radiating, in that the inverse r dependence predominates.

Figure A-1. Dipole *p* and *E*-field components.

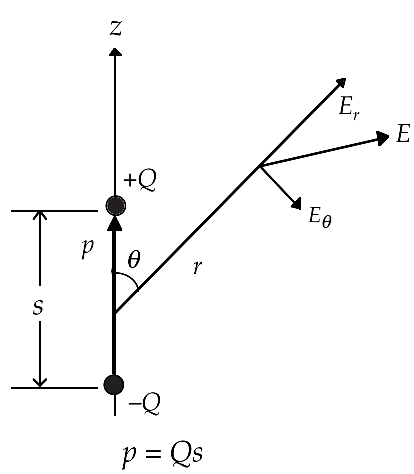

*W. Panofsky and M. Philips, *Classical Electricity and Magnetism*, Reading, MA, Addison-Wesley Publishing Company, Inc., 1962, p. 258.

Three observation zones are defined by Kelly, depending on the observation distance *r* and the wavelength λ relative to the extent *D* of the source region.

The static zone is for the observation point between the source region and one wavelength away, or

$$D \ll r \ll \lambda \ . \qquad \text{(A-4)}$$

This expression, *r* is much greater than *D*, is valid in most every case if the sources are atoms and molecules. The wavelength is much greater than the observation distance for frequencies of 300 kHz or less for the ranges of 0.1 to 10 km, which is a distance at which a soldier in the field might want to detect an artillery launch or detonation. We therefore would expect the dipole terms and transition terms to predominate. That is, we would expect a large radial field and a large transverse field. The large radial field compared to the transverse field does not reduce the detectability of the signal, but these two signals combine to produce a larger measured field nearer the source than we would expect by measuring only the transverse component of the field. Therefore the extrapolation of measurements of the *E*-field near the source to far-field expectations, as was done in section 2.15.1, would overestimate the far-field.

The induction zone is for the observation to be on the order of a wavelength away from the source:

$$D \ll \lambda \approx r \ . \qquad \text{(A-5)}$$

This expression means that λ and *R* are much greater than the source region. Thus the observation distance (on the order of the wavelength) of 0.1 to 10 km would correspond to frequencies between 3 and 30 kHz.

The radiation zone corresponds to distances much greater than a wavelength away from the source:

$$D \ll \lambda \ll r \ . \qquad \text{(A-6)}$$

Classifying measured *E*-fields as radiation fields therefore requires consideration of the wavelength (or frequency), distance from source to observation point, and size of source, in order to ensure that the radial field component is negligibly small compared to the transverse field component. When these criteria are applied to most of the data in the literature reported in the text, section 2, especially Trinks,* section 2.1, the observations are found to be made in the near field, where a considerable radial component of the *E*-field exists, and not in the far-field, as most of the authors claim.

---

*H. Trinks, "Electrical Charge and Radiation Effects Near Projectiles and Fragments," Harry Diamond Laboratories, R-850-76-1, September 1976.

Distribution

Admnstr
Defns Techl Info Ctr
Attn DTIC-OCP
8725 John J Kingman Rd Ste 0944
FT Belvoir VA 22060-6218

Defns Threat Reduction Agency
Attn SWP-1 E Rinehart
Attn SWTI A Verna
Attn SWTI G Lu
1680 Texas Street, S.E.
Kirtland AFB NM 87117-5669

Defns Threat Reduction Agency (DTRA)
Attn CPA S E Dains
Attn PMP-ATC G Baker (2 copies)
6801 Telegraph Rd
Alexandria VA 22310-3398

Ofc of the Dir Rsrch and Engrg
Attn R Menz
Pentagon Rm 3E1089
Washington DC 20301-3080

Ofc of the Secy of Defns
Attn ODDRE (R&AT)
Attn ODDRE (R&AT) S Gontarek
The Pentagon
Washington DC 20301

OSD
Attn OUSD(A&T)/ODDDR&E(R) R J Trew
Washington DC 20301-7100

PEO-Theater Air Defns National Ctr
Attn 2/9W62 D Marker, Technology Dir
2531 Jefferson Davis Highway
Arlington VA 22242-5170

AMCOM MRDEC
Attn AMSMI-RD W C McCorkle
Redstone Arsenal AL 35898-5240

CECOM
Attn PM GPS COL S Young
FT Monmouth NJ 07703

Dir for MANPRINT
Ofc of the Deputy Chief of Staff for Prsnnl
Attn J Hiller
The Pentagon Rm 2C733
Washington DC 20301-0300

Hdqtrs Dept of the Army
Attn DAMO-FDT D Schmidt
400 Army Pentagon Rm 3C514
Washington DC 20301-0460

Ofc of the Proj Mgr for Mines, Countermines, & Demltn
Attn AMCPM-DSA-MCD T Hoffman
Attn AMCPM-TDS-MC R Andrejkovics
Picatinny Arsenal NJ 07806-5000

US Army Edgewood RDEC
Attn SCBRD-TD G Resnick
Aberdeen Proving Ground MD 21010-5423

US Army Info Sys Engrg Cmnd
Attn ASQB-OTD F Jenia
FT Huachuca AZ 85613-5300

US Army Natick RDEC
Acting Techl Dir
Attn SSCNC-T P Brandler
Natick MA 01760-5002

Director
US Army Rsrch Ofc
4300 S Miami Blvd
Research Triangle Park NC 27709

US Army Simulation, Train, & Instrmntn Cmnd
Attn J Stahl
12350 Research Parkway
Orlando FL 32826-3726

US Army Sp & Strtgc Defns Cmnd
Attn CSSD-TC-ST K Blankenship
PO Box 1500
Huntsville AL 35807-3801

US Army Tank-Automtv & Armaments Cmnd
Attn AMSTA-AR-TD M Fisette
Bldg 1
Picatinny Arsenal NJ 07806-5000

US Army Tank-Automtv Cmnd Rsrch, Dev, & Engrg Ctr
Attn AMSTA-TA J Chapin
Warren MI 48397-5000

Distribution (cont'd)

US Army Train & Doctrine Cmnd Battle Lab
Integration & Techl Dirctrt
Attn ATCD-B J A Klevecz
FT Monroe VA 23651-5850

Commander-in-Chief
Atlantic Fleet
Attn Code N-8 R Whiteway
1562 Mitscher Avenue
Norfolk VA 23551

Nav Rsrch Lab
Attn Code 6650 T Wieting
4555 Overlook Ave SW
Washington DC 20375-5000

Nav Surface Warfare Ctr
Attn Code B07 J Pennella
17320 Dahlgren Rd Bldg 1470 Rm 1101
Dahlgren VA 22448-5100

Naval Air Warfare Ctr
Unconventional Observables/
Techl Oversight Ofc
Attn Code 526E00D D Schriner
China Lake CA 93555-6001

Naval Air Warfare Ctr Weapons Div
Attn Code 474330D H John, Jr.
Attn T M Atienza-Moore
China Lake CA 93555-6001

Lawrence Livermore Natl Lab
Attn L228 J Morrison
Attn L282 J Reaugh
Attn L282 M Murphy
PO Box 808
Livermore CA 94551-5554

Los Alamos Natl Lab
Attn DX3 L Hull
Mail Stop P940
Los Alamos NM 87545

Los Alamos Natl Lab
Attn DARHT E Pogue
Mail Stop P941
Los Alamos NM 87545

Los Alamos Natl Lab
Attn DOD K F McKenna
Mail Stop F613
Los Alamos NM 87545

Los Alamos Natl Lab
Attn NW/CWT J V Repa
Mail Stop F613
Los Alamos NM 87545

Los Alamos Natl Lab
Attn P22 R E Kelly
Mail Stop D410
Los Alamos NM 87545

DARPA
Attn B Kaspar
3701 N Fairfax Dr
Arlington VA 22203-1714

Hicks & Associates, Inc
Attn G Singley III
1710 Goodrich Dr Ste 1300
McLean VA 22102

Laboratory for Physical Sciences
Attn A J Leyendecker, PH.D. Senior Scientist
8050 Greenmead Drive
College Park MD 20740

Palisades Inst for Rsrch Svc Inc
Attn E Carr
1745 Jefferson Davis Hwy Ste 500
Arlington VA 22202-3402

US Army Rsrch Lab
Attn AMSRL-D R W Whalin
Attn AMSRL-DD J Rocchio
Attn AMSRL-CI-LL Techl Lib (3 copies)
Attn AMSRL-CS-AS Mail & Records Mgmt
Attn AMSRL-CS-EA-TP Techl Pub (3 copies)
Attn AMSRL-SE J M Miller
Attn AMSRL-SE J Pellegrino
Attn AMSRL-SE-DE J Miletta
Attn AMSRL-SE-DE L Libelo
Attn AMSRL-SE-DE R Chase
Attn AMSRL-SE-DP M Litz

Distribution (cont'd)

US Army Rsrch Lab (cont'd)
Attn AMSRL-SE-DS L Jasper
Attn AMSRL-SE-RS A Sindoris
Attn AMSRL-SE-RU B Scheiner
Attn AMSRL-SE-RU M Ressler
Attn AMSRL-SE-SA J Eicke
Attn AMSRL-SE-SS D Hull (5 copies)
Attn AMSRL-SE-SS J Chopack

US Army Rsrch Lab (cont'd)
Attn AMSRL-SE-SS J Fine (30 copies)
Attn AMSRL-SE-SS J Hopkins
Attn AMSRL-SE-SS M Kolodny
Attn AMSRL-SE-SS S Vinci (10 copies)
Attn AMSRL-SE-SS V Marinelli
Attn AMSRL-SE-SS H Leupold
Attn C Campagnuolo
Adelphi MD 20783-1197

REPORT DOCUMENTATION PAGE

Form Approved
OMB No. 0704-0188

1. AGENCY USE ONLY *(Leave blank)*

2. REPORT DATE December 1998

3. REPORT TYPE AND DATES COVERED Interim, 12/95 to 12/97

4. TITLE AND SUBTITLE Causes of Electromagnetic Radiation From Detonation of Conventional Explosives: A Literature Survey

5. FUNDING NUMBERS
DA PR: AH16
PE: 62120A

6. AUTHOR(S) Jonathan E. Fine and Stephen J. Vinci

7. PERFORMING ORGANIZATION NAME(S) AND ADDRESS(ES)
U.S. Army Research Laboratory
Attn: AMSRL-SE-SS email: jfine@arl.mil
2800 Powder Mill Road
Adelphi, MD 20783-1197

8. PERFORMING ORGANIZATION REPORT NUMBER
ARL-TR-1690

9. SPONSORING/MONITORING AGENCY NAME(S) AND ADDRESS(ES)
U.S. Army Research Laboratory
2800 Powder Mill Road
Adelphi, MD 20783-1197

10. SPONSORING/MONITORING AGENCY REPORT NUMBER

11. SUPPLEMENTARY NOTES
ARL PR: 7NE4TR
AMS code: 622120.H1611

12a. DISTRIBUTION/AVAILABILITY STATEMENT Approved for public release; distribution unlimited.

12b. DISTRIBUTION CODE

13. ABSTRACT *(Maximum 200 words)*

A literature survey was conducted on the presence of electromagnetic radiation from the detonation of conventional explosives. This survey is part of a technology effort to identify a useful battlefield signature that an individual soldier could detect. Sources reported observations of such signals in the range from as low as 0.5 Hz up to 2 GHz. Several of the investigators believed that the likeliest cause was charged particles created by ionization within the explosive region. The frequencies of the radiation appear related to the duration of shock waves and other hydrodynamic phenomena caused by the detonation. A calculation model presented in the literature provides estimates of frequency bands in this range and also of signal levels produced. The model is used to analyze some of the published results and provide some correlation between observations of several investigators.

14. SUBJECT TERMS
Explosion sensor, rf from explosions, rf signature, shock wave radiation, explosion radiation, explosion signature, detonation radiation, electromagnetic signature of explosions, electromagnetic signature of detonations, projectile detonation verification

15. NUMBER OF PAGES 50

16. PRICE CODE

17. SECURITY CLASSIFICATION OF REPORT	18. SECURITY CLASSIFICATION OF THIS PAGE	19. SECURITY CLASSIFICATION OF ABSTRACT	20. LIMITATION OF ABSTRACT
Unclassified	Unclassified	Unclassified	UL

NSN 7540-01-280-5500

Standard Form 298 (Rev. 2-89)
Prescribed by ANSI Std. Z39-18
298-102

DEPARTMENT OF THE ARMY
U.S. Army Research Laboratory
2800 Powder Mill Road
Adelphi, MD 20783-1197